



# QCD and symmetries related to nucleon structure and strongly interacting matter

G. Chanfray

## ► To cite this version:

G. Chanfray. QCD and symmetries related to nucleon structure and strongly interacting matter. École thématique. Ecole Joliot Curie 2010, Lacanau, 2010, pp.45. cel-00760885

**HAL Id: cel-00760885**

**<https://cel.hal.science/cel-00760885>**

Submitted on 4 Dec 2012

**HAL** is a multi-disciplinary open access archive for the deposit and dissemination of scientific research documents, whether they are published or not. The documents may come from teaching and research institutions in France or abroad, or from public or private research centers.

L'archive ouverte pluridisciplinaire **HAL**, est destinée au dépôt et à la diffusion de documents scientifiques de niveau recherche, publiés ou non, émanant des établissements d'enseignement et de recherche français ou étrangers, des laboratoires publics ou privés.

# QCD and Symmetries related to nucleon structure and strongly interacting matter.

G. Chanfray

*Institut de Physique Nucléaire de Lyon*

*Université de Lyon, Université Lyon 1 et IN2P3-CNRS , F-69622 Villeurbanne Cedex*

## Abstract

We discuss the impact of the symmetries of Quantum ChromoDynamics (QCD) on the observed properties of hadrons and strongly interacting matter. We first introduce the fundamental color gauge symmetry insisting on its non perturbative aspect at low energy. Particular emphasis is put on the spontaneous breaking of chiral symmetry and its numerous consequences. Operational approaches, such as chiral perturbation theory or QCD sum rules, allowing to implement this crucial symmetry at the hadronic level are presented. We then explore the consequences of chiral restoration at finite baryonic density and/or temperature on the properties of in-medium hadrons in connection with experimental programs. Finally we give a short discussion of the phase structure of QCD in connection with chiral symmetry and the center symmetry associated with the confinement/deconfinement transition.

## 1 Introduction

The aim of these lectures is to discuss the symmetry properties of Quantum ChromoDynamics (QCD) which is now commonly accepted as the theory of strong interaction. More precisely we will show that these symmetries can be utilized as a guide for the understanding of strong interaction physics to be confronted with experimental observations. This concerns in first rank the elementary excitations of the QCD ground state, namely the hadron spectrum, the description of ordinary nuclear matter as well as the phase structure of QCD at high temperature and/or baryonic density.

The basic symmetry of QCD is the color symmetry. Each fundamental particle of QCD, the quark, can exist in three different color states. Any transformation among color states should leave the theory invariant. The mathematical realization of these transformations defines a group of  $SU(3)_{color}$  “gauge” transformations. Moreover this invariance has to be local : the theory is invariant if one transforms the color states independently at different space-time points which implies that a connection must exist between these different points. This connection or interaction between quarks is carried by eight gluons. The situation is similar to the exchange of neutral photons between electrically charged particles but there is a major difference since the gluons themselves carry a color charge and they interact with each other. This is certainly the main origin of (what should be) the most crucial property, named color confinement, of the resulting gauge quantum field theory. Isolated quarks have never been observed and the only existing hadrons are uncolored or “white” objects with typical mass of  $1\text{ GeV}$  and typical size of order  $1\text{ fm}$ .

In the low energy domain only light  $u$  and  $d$  quarks with masses of a few  $\text{MeV}$ 's are involved. In this range the QCD lagrangian has essentially no dimensional parameter. This scale invariance is however broken by quantum fluctuations. The consequence is that the coupling constant of the theory depends on the momentum scale at which the interacting quarks and gluons are probed. It turns out that due to the gluon self-interactions this effective or running coupling constant decreases with increasing momentum: this is the famous asymptotic freedom of QCD. Conversely at low momentum the coupling constant may become very large and QCD becomes a fully non perturbative theory which is supposed to generate color confinement. The scale associated with the non perturbative regime,  $\Lambda_{QCD} = 200\text{ MeV}$ , is the parameter of the theory and is fixed by analysis of experimental data. The corresponding length scale,  $\hbar c/\Lambda_{QCD} = 1\text{ fm}$ , coincides with the typical hadronic size. More generally all low energy QCD observables, such as hadron masses, are just proportional to  $\Lambda_{QCD}$  with the appropriate power, the numerical constant being given by the non perturbative QCD dynamics. The non perturbative quantum fluctuations also generate a gluon condensate directly related to the energy density of the QCD ground state (or QCD vacuum).

As said previously the fundamental color symmetry is not directly visible in the hadron spectrum. There is however another symmetry which is accidental in the sense that it is linked to the very small mass difference between  $u$  and  $d$  quark of the order of a few  $MeV$ 's. The QCD lagrangian is almost exactly invariant under global  $SU(2)$  transformations acting on  $u$  and  $d$  quarks independently of their colors. This is the venerable isospin or vector symmetry. The observational consequence is the existence of isospin multiplets made of hadrons with almost exactly the same mass. Well known examples are the doublet of nucleons, or the triplets of  $\pi$  or  $\rho$  mesons. In reality, not only the mass difference but also the absolute values of the  $u$  and  $d$  quark masses are very small. This results in another global symmetry named axial symmetry. The vector and axial symmetries can be combined into the chiral  $SU(2)_L \otimes SU(2)_R$  symmetry acting separately on left- and right- handed quarks. However the absence of degenerate chiral partners with opposite parity indicates that the chiral symmetry is spontaneously broken. The QCD ground state is not invariant under axial transformations and possesses a large scalar density of quark-antiquark pairs generating the so-called quark condensate. One direct observational evidence of the spontaneous symmetry breaking is the existence of soft (low mass) Goldstone particles identified with the light pions. These symmetry considerations can be extended to the strange sector although the resulting  $SU(3)_L \otimes SU(3)_R$  symmetry is less accurate.

It is expected that chiral symmetry is progressively restored when the baryonic density and/or the temperature increase, one consequence being the dropping of the quark condensate and the pion decay constant. One key question is to relate this gradual restoration to the evolution of hadron properties or more precisely to the modification of the hadron spectral functions, in particular those associated with chiral partners. An important example is provided by the  $\rho$  meson and the axial-vector meson  $a_1$ . Although chiral symmetry breaking and its restoration can be studied by numerical simulations on a lattice, it is useful to study it with models, a very popular one being the Nambu-Jona-Lasinio model and its extensions. There are also operational approaches which allow to implement chiral symmetry directly at the hadronic level. It is for instance possible to reformulate low energy QCD directly in terms of hadron degrees of freedom to study the dynamics of low momentum pions and their coupling to light baryons. This is the famous chiral perturbation theory (ChPT) which successfully describes many low energy processes and constitutes a basis for the description of nuclear matter at not too high density. Another approach, which is also in principle model independent, is based on QCD sum rules (QCDSR). It allows to relate the hadron spectral functions (in short mass and width) to the fundamental gluon and quark condensates. One important point is the possibility of extending the QCDSR at finite density and to relate the evolution of the hadron properties to the modification of the QCD vacuum through the modification (dropping) of the QCD condensates. This constitutes one major way for addressing the important question of in-medium hadrons which has motivated numerous theoretical works as well as an important experimental activity. The very prominent example is the rho meson. An important broadening of the  $\rho$  has been observed in dilepton production off relativistic heavy ion collisions by the NA60 collaboration. The important theoretical challenge of this domain is to identify physical mechanisms associated with chiral restoration which are compatible with experimental data and many-body hadronic calculations.

Full chiral symmetry restoration at high density and/or temperature means a change of the symmetry pattern associated with a different QCD phase in the thermodynamic language. Indeed lattice calculations show a sudden decrease of the quark condensate (playing the role of an order parameter) in a narrow temperature window around  $T_C = 180 MeV$  which is accompanied by a simultaneous increase of thermodynamic quantities (such as the energy density). This is attributed to the liberation of the most numerous quark and gluon degrees of freedom, indicating a confinement/deconfinement transition. The conclusion which can be drawn from the analysis of experimental data at SPS and RHIC is that the phase boundary is really traversed in relativistic nucleus-nucleus collisions. The details of the phase structure and the nature of the chiral transition depend on the quark masses. For physical quark masses a first order transition is expected at non vanishing baryonic chemical potential and a critical end point (CEP) is predicted. Its experimental search is one of the central goal of the FAIR-CBM and of the RHIC-Energy-Scan project. It also exists a symmetry aspect which is behind confinement. This symmetry, named center symmetry, is nonetheless valid only for the pure glue theory. However even in the presence of dynamical quarks the associated order parameter, the Polyakov loop, remains an indicator of the deconfinement as demonstrated by lattice simulations or model calculations reproducing the QCD thermodynamics, such

as the polyakov-NJL model. Simultaneous studies of chiral restoration and deconfinement can be also performed by looking at the evolution of the quark condensate and the Polyakov loop.

These lectures are divided in four parts along the lines given above. In section 2 we give a brief overview of QCD and section 3 is devoted to a rather detailed discussion of chiral symmetry. In section 4 we discuss some successful approaches, chiral perturbation theory and QCD sum rules, which largely utilize the symmetries properties of QCD to describe the hadron spectrum, strongly interacting matter and the in-medium behavior of hadrons. Finally the last section deals with QCD thermodynamics in connection with relativistic heavy ion collisions. Throughout these lectures we use the natural system of units where  $\hbar = c = 1$ . In this system there is only one type of dimension :  $[Energy] = [Momentum] = [Length]^{-1} = [Time]^{-1}$ . The connection with an usual system of units is done by taking  $\hbar c = 197.3 \text{ MeV} \cdot \text{fm}$ . Hence if one finds for the energy of a system with size  $R$  the result  $E = k/R$ , ( $k$  being some dimensionless constant of order unity) it has to be understood as  $E = k \hbar c / R$ . It follows that in practice  $E (\text{MeV}) = k \cdot 197.3 / R (\text{fm})$  or  $1 \text{ fm}^{-1} = 197.3 \text{ MeV} \approx 200 \text{ MeV}$ . There are several textbooks or review articles devoted to QCD. I give here two references [1, 2] that I personally use.

## 2 Overview of QCD

### 2.1 QCD as a SU(3) gauge theory

**Historical introduction : the rationale for QCD.** At the beginning of the sixties it has been realized that all the known hadrons could be built with basic building blocks called quarks [3]. At this epoch, only three quark flavors (u,d,s) were needed and the baryons appeared as made of three quarks and the mesons made of a quark and an antiquark. However despite the important phenomenological successes some conceptual problems were present : among them the existence of objects such as the  $\Delta^{++}$  in the spin state  $m_s = 3/2$ . Such a configuration made of three identical  $u$  quarks in the same spin-up state clearly violates the Pauli principle. To solve this problem it was postulated that each quark in a given flavor can possess three distinct color charges ( $i = 1, 2, 3$  or red, yellow, blue). In this proposed scheme the hadrons have in addition to be color singlets : they are “white”. Mathematically this means that the hadron configurations are invariant under a unitary matrix transformation with unit determinant (to eliminate an irrelevant global phase) acting on quark color coordinates :  $q_i \rightarrow V_{ik} q_k$  with  $V^\dagger V = 1$  and  $\det V = 1$ . This defines the group of  $SU(3)_c$  matrices of the form  $V = \exp(i\theta_a t_a)$  where the  $\theta_a$  are eight continuous real parameters and the eight generators  $t_a$  are related to the Gell-mann matrices by  $t_a = \lambda_a/2$ . The only irreducible possible singlet representations are

$$3_c \times 3_c \times 3_c \quad (\text{baryons}) \quad 3_c \times \bar{3}_c \quad (\text{mesons})$$

in agreement with the experimental observations. The color space baryon wave function writes

$$B = \sum_{i,j,k=1}^3 \epsilon_{ijk} q_i q_j q_k \quad (1)$$

which is fully antisymmetric under color exchange. Coming back to our previous example, the  $m_s = 3/2$ ,  $\Delta^{++}$  state writes  $\Delta^{++} = \sum_{i,j,k} \epsilon_{ijk} u_i \uparrow u_j \uparrow u_k \uparrow$ . Similarly a meson state has the form in color space :

$$M = \sum_i q_i \bar{q}_i = R\bar{R} + Y\bar{Y} + B\bar{B}. \quad (2)$$

To go beyond this very ad-hoc construction the next step has been to build a dynamical theory of color whose consequences should be the non existence of quarks as free particle and the only existence of white hadrons with typical size of  $1 \text{ fm}$  and typical mass of  $1 \text{ GeV}$ . This property is called color confinement. This theory has progressively emerged as a  $SU(3)_c$  gauge theory.

**Building of the gauge theory.** Such a theory is based on a “local gauge invariance principle”. To a large extent, given the gauge group, the structure of the lagrangian can be obtained. We show below

how this can be done. As a starting point let us consider a free fermion (quark) theory whose lagrangian density is :

$$\mathcal{L} = i \bar{\psi} \gamma^\mu \partial_\mu \psi - m \bar{\psi} \psi \quad \text{with} \quad \psi = \begin{pmatrix} \psi_1 \\ \psi_2 \\ \psi_3 \end{pmatrix} \quad \bar{\psi} = \psi^\dagger \gamma^0 = (\bar{\psi}_1, \bar{\psi}_2, \bar{\psi}_3). \quad (3)$$

For the moment we consider one flavor of quark and the field  $\psi_i$  represents the quark with color  $i$ . The gauge principle requires that the lagrangian has to be invariant under a local gauge transformation where the continuous parameter,  $\theta_a(x)$ , is now a function of space-time :

$$\psi(x) \rightarrow V(x) \psi(x) \quad \text{with} \quad V(x) = e^{i\theta_a(x) T_a}. \quad (4)$$

This invariance is clearly not realized due to the presence of a derivative in the lagrangian. To examine this point in a more detailed way, let us discretize the theory on a four-dimensional lattice with lattice spacing  $a$  (see fig. 1). We note  $e_\mu, \mu = 0, 1, 2, 3$ , the unit vectors along the four space-time axis (we do not distinguish between Minkovski and Euclidean metrics). In the kinetic energy piece of the lagrangian the derivative becomes a difference :

$$\mathcal{L}_K = i \bar{\psi} \gamma^\mu \partial_\mu \psi = \frac{i}{a} \sum_\mu \left( \bar{\psi}(x) \gamma^\mu \psi(x + a e_\mu) - \bar{\psi}(x) \gamma^\mu \psi(x) \right).$$

Only the first term, which is non local, is non invariant since the  $V^\dagger$  and  $V$  matrices are taken at different space-time points :

$$\bar{\psi}(x) \gamma^\mu \psi(x + a e_\mu) \rightarrow \bar{\psi}(x) \gamma^\mu V^\dagger(x) V(x + a e_\mu) \psi(x + a e_\mu). \quad (5)$$

To obtain a gauge invariant theory it is necessary to include some kind of connection between different space-time points. For this reason one introduces new degrees of freedom,  $U(x; y)$ , called link variables, which are also elements of the gauge group and satisfy the very natural conditions :  $U(x; x) = 1$ ,  $U^{-1}(x; y) = U(y; x)$ . The non invariant piece of the lagrangian is modified according to

$$\mathcal{L}_K = \frac{i}{a} \sum_\mu \left( \bar{\psi}(x) \gamma^\mu U(x; x + a e_\mu) \psi(x + a e_\mu) - \bar{\psi}(x) \gamma^\mu \psi(x) \right) \quad (6)$$

which is gauge invariant provided the link variables transform as  $U(x; y) \rightarrow V(x) U(x; y) V^\dagger(y)$ . The elementary link variable being an element of the gauge group it has to be of the form  $U(x, x + a e_\mu) = e^{iB_\mu^a} = 1 + iaB_\mu^a + \mathcal{O}(a^2)$  with  $B^\mu(x) = B_a^\mu(x) t^a$ . This defines eight gluon fields,  $B_a^\mu(x)$ . Taking the continuum limit ( $a \rightarrow 0$ ), one obtains the transformation law for the gauge fields,  $B_\mu(x) \rightarrow V(x) B_\mu(x) V^\dagger(x) - iV(x) \partial_\mu V^\dagger(x)$ , and the form of the lagrangian :

$$\mathcal{L} = \bar{\psi}(x) \gamma_\mu \left( i\partial^\mu - t_a B_a^\mu(x) \right) \psi(x) - m \bar{\psi}(x) \psi(x). \quad (7)$$

At this level the glue field has no dynamical content. The simplest kinetic or potential term is the so-called plaquette term depicted on the middle panel of fig. 1

$$\mathcal{L}_J = \frac{1}{g^2 a^4} \sum_{(\mu, \nu)} \text{tr}(U_{12} U_{23} U_{34} U_{41}) \quad (10.2.12)$$

where  $g$  will be identified with the (strong) coupling constant and the  $1/a^4$  term ensures the correct dimension. Thanks to the cyclic properties of the (color) trace, this plaquette lagrangian is obviously gauge invariant. Taking again the  $a \rightarrow 0$  limit, the continuum limit lagrangian is obtained. The full QCD lagrangian is obtained by summing on all possible quark flavors  $f$  in the kinetic and mass quark pieces with the adjunction of the plaquette lagrangian

$$\mathcal{L}_{\text{QCD}} = \sum_f \bar{\psi}_f \gamma_\mu (i\partial^\mu - g t_a A_a^\mu) \psi_f - \sum_f m_f \bar{\psi}_f \psi_f - \frac{1}{4} G_{\mu\nu}^a G_a^{\mu\nu} \quad (8)$$

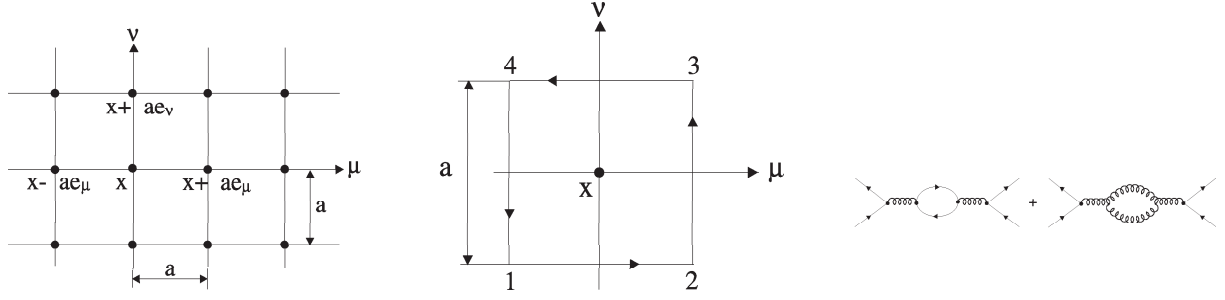


Figure 1: Left panel : discretized Euclidean space. Middle panel : plaquette term; the arrows indicate the direction of the links. Right panel :  $q\bar{q}$  and gluon loop corrections to gluon exchange between quarks. Each vertex is weighted by the coupling constant  $g$ .

where the canonical gluon field  $A^\mu$  is defined by  $B^\mu = gA^\mu = g \sum_{a=1}^{N_c^2-1} t_a A_a^\mu$ . The last term represents the continuum limit of the plaquette term. It involves the gluon field tensor :

$$\begin{aligned} G^{\mu\nu} &= \partial^\mu A^\nu - \partial^\nu A^\mu + ig[A^\mu, A^\nu] \equiv t_a G_a^{\mu\nu} \\ G_a^{\mu\nu} &= \partial^\mu A_a^\nu - \partial^\nu A_a^\mu - g f_{abc} A_b^\mu A_c^\nu. \end{aligned} \quad (9)$$

The  $f_{abc}$  coefficients are the fully antisymmetric structure constants originating from the  $SU(3)$  Lie algebra  $[t_a, t_b] = i f_{abc} t_c$ . There is a standard Yukawa coupling term of the glue to the quarks which is the exact analog of the Yukawa coupling of the electromagnetic field to electrons in QED. The new feature peculiar to the non abelian QCD theory is the existence of the term  $g f_{abc} A_b^\mu A_c^\mu$  in the gluon strength tensor. By inspection of the lagrangian (8) we see that it generates three- and four-gluon interactions weighted by  $g$  and  $g^2$ . The gluons have self-interactions since they also carry a color charge at variance with photons in QED which are electrically neutral. This feature has very profound consequences as we will see below. From the lagrangian it is evidently possible to derive Feynman rules and develop a standard perturbation approach for scattering processes. However such an approach will be meaningful only for high momentum transfer (short range) interactions since, due to renormalization as explained below, QCD is realized in a fully non perturbative way in the low energy-momentum domain corresponding to the fermi scale.

## 2.2 Breaking of scale invariance; running coupling constant

The masses of the quarks entering the QCD lagrangian cover a very large domain :  $m_u \simeq 5 \text{ MeV}$ ,  $m_d \simeq 9 \text{ MeV}$ ,  $m_s \simeq 150 \text{ MeV}$ ,  $m_c \simeq 1.5 \text{ GeV}$ ,  $m_b \simeq 4.5 \text{ GeV}$ ,  $m_t \simeq 175 \text{ GeV}$ . In the low energy domain of interest the heavy quarks are frozen and we only have to consider the light quarks, essentially  $u$  and  $d$ , and also to a less extent the strange quark. The important point is that the light quarks are indeed extremely light; their masses are essentially compatible with zero as compared to typical hadron masses of the order of  $1 \text{ GeV}$ . We can conclude that the QCD lagrangian restricted to the light quark sector has (almost) no scale since it involves only a dimensionless parameter, the coupling constant  $g$ . In the following the  $m_{u,d} = 0$  case, corresponding to exact scale invariance, will be referred as the chiral limit (the reason of this terminology will be given in section 3).

It is however important to realize that from the very nature of a quantum field theory (QFT), the presence of quantum fluctuations of arbitrary size explicitly breaks scale invariance. In other words a QFT should be defined at each momentum scale  $\mu$  (or at each space-time resolution  $1/\mu$ ). For that reason one defines an effective or running coupling constant  $g(\mu)$  for each scale  $\mu$ . This effective coupling constant contains by definition the effect of quantum fluctuations of high momentum  $k > \mu$  (or size smaller than  $1/\mu$ ). To clarify this very crucial notion let us take the example of quark-quark scattering. To leading order in perturbation theory, it is described by a single gluon exchange and the amplitude goes like  $g^2$ . However during its path from one quark to the other quark, the gluon may very well fluctuate into virtual pairs of quark and gluons which is allowed by the Heisenberg uncertainty principle as depicted on the right panel of fig. 1. Such contributions of order  $g^4$  are perfectly calculable using standard Feynman rules derived

from the QCD lagrangian. If the (space-like) exchanged momentum is  $q$ , it is convenient to consider the QFT formulated at a scale  $\mu$  close to  $Q = \sqrt{-q^2} = \sqrt{q^2 - q_0^2}$ . To calculate the corrected scattering amplitude we proceed qualitatively as follows : we divide the contributions of quantum fluctuation momenta (the momentum  $k$  running into the quark or gluon loop appearing in fig. 1) into those smaller than  $\mu$  and those larger than  $\mu$ . The small momentum fluctuations are treated as normal fluctuations and the larger ones are absorbed in the definition of the coupling constant  $g(\mu)$ . When going from one scale  $\mu + \delta\mu$  to the scale  $\mu$ , the quantum fluctuations with momenta between  $\mu$  and  $\mu + \delta\mu$  originally not included in the definition of  $g(\mu + \delta\mu)$  are incorporated in the definition of  $g(\mu)$ . This procedure is called the renormalization. It follows implicitly that there is a one to one correspondence between the coupling constant of the theory and the scale (renormalization point)  $\mu$ . To characterize the evolution law we define the Gell-Mann beta function :

$$\beta(g) = \mu \frac{dg}{d\mu} \equiv \frac{dg}{d \ln \mu}. \quad (10)$$

It is important to notice that this beta function is an intrinsic property of the theory (QCD) and is a function of the coupling constant  $g$  only. Hence  $\beta(g)$  being given the evolution of  $g$  can be calculated using the above relation (10) known as the Callan-Symanzik equation. In the perturbative regime where  $g$  is small,  $\beta(g)$  can be calculated with the result  $\beta(g) = -\beta_0 g^3 + \beta_1 g^5 + \dots$ . The important point is that  $(4\pi)^2 \beta_0 = \frac{11}{3} N_c - \frac{2}{3} N_f$  is always positive for  $N_c = 3$ , whatever the number of flavors,  $N_f$ , is. This means that  $g(\mu)$  is a decreasing function of  $\mu$  and  $g = 0$  where  $\beta(g) = 0$  is a true minimum of the function  $g(\mu)$ . Consequently when the momentum scale  $\mu$  increases,  $g$  will be “attracted” near the point  $g = 0$  which is said to be an attractive ultraviolet fixed point. Hence at very high momentum scales, or for very short distances, the coupling constant goes to zero and QCD behaves like a free field theory. This property is called asymptotic freedom. In the high momentum domain we can keep only the leading contribution to  $\beta(g)$ . Explicit integration of the Callan-Symanzik equation (10) yields

$$\mu = \Lambda \exp \left( \frac{1}{2\beta_0 g^2} \right) (\beta_0 g^2)^{-\beta_1/2\beta_0} \quad (11)$$

where  $\Lambda$  is a certain mass scale which is a priori unknown.

Suppose that we want to calculate in QCD an observable with dimension  $D$  (for instance  $D = 1$  for a hadron mass). We start by formulating the theory at a certain (a priori arbitrary) scale  $\mu$ . Since the QCD lagrangian in the chiral limit has no scale, all the dimensional physical quantities must be expressed in term of the renormalization scale  $\mu$  with power  $D$ . From dimensional analysis this observable  $O$  has thus to be of the form  $O = \mu^D f(g(\mu))$  where  $f(g)$  is a dimensionless function. However the numerical value of this observable has to be independent of  $\mu$ . Hence one must have :

$$\frac{dO}{d\mu} \equiv 0 \quad \Rightarrow \quad D f + \mu \frac{df}{dg} \frac{dg}{d\mu} = 0 \quad \Rightarrow \quad \frac{df}{f} = -D \frac{dg}{\beta(g)}. \quad (12)$$

Explicit integration in the perturbative domain gives

$$O = C \mu^D \exp \left( \frac{-D}{2\beta_0 g^2} \right) (\beta_0 g^2)^{D\beta_1/2\beta_0} \quad (13)$$

where  $C$  is a numerical dimensionless constant. Combining eq. (11) and (13), the arbitrary scale  $\mu$  can be eliminated in favor of  $\Lambda$ . It follows that:

$$O = C \Lambda_{QCD}^D. \quad (14)$$

The quantity  $\Lambda$ , now called  $\Lambda_{QCD}$ , appears as the fundamental scale of QCD. Each physical observable (associated with light quarks) of QCD has to be proportional to this scale with the appropriate power equal to its dimension. Solving QCD thus reduces to calculate the various constants  $C$ . This is what is done in numerical lattice simulations. The system is discretized and the fields exist only at discrete points. What plays the role of the scale is obviously  $\mu = 1/a$  where  $a$  is the lattice spacing. Hence when calculating an observable, what is really obtained is the dimensionless quantity  $O a^D$  and the result is

a function of  $g$  only. Once this is done one looks at the behaviour of the numerical results with  $g$  and check the low  $g$  scaling (eq. 13) and the constant  $C$  can be extracted. One important lesson is that the origin of ordinary hadrons (nucleons) mass scale is the scale  $\Lambda_{QCD}$ . It appears as a parameter of the theory and has to be extracted from experimental data. To see this point let us consider deep inelastic lepton (electron for instance) scattering on the proton which has revealed its quark-parton structure [2]. The exchanged virtual photon emitted by the electron carries a space-like momentum  $q$  and probes the distribution of quark-partons at momentum scale  $\mu = Q$ , or space-time resolution  $1/Q$ . Said differently the virtual photon probes a (weakly interacting) QCD system where quarks and gluons interact with coupling constant  $g(\mu = Q)$ . Inversing eq. (11), its explicit form at very high  $Q$  is given by :

$$g^2(Q^2) = \frac{1}{\beta_0 \ln(Q^2/\Lambda_{QCD}^2)} \quad (15)$$

It is also clear that high  $Q$  means  $Q$  much larger than the fundamental scale  $\Lambda_{QCD}$ . Varying experimentally  $Q$  allows to study the evolution law for  $g^2(Q^2)$  and thus to extract the numerical value of the fundamental scale. The result is  $\Lambda_{QCD} \simeq 200 \text{ MeV}$  and the associated length scale is  $R_H = 1/\Lambda_{QCD} \simeq 1 \text{ fm}$ . For momentum scale below  $\Lambda_{QCD}$ , or size of the order  $R_H$ , QCD becomes totally non perturbative. It can be noticed that  $R_H$  corresponds to the typical light hadrons size. This also implies that the problem of hadron structure is by essence a totally non perturbative problem.

### 2.3 Trace anomaly and gluon condensate; vacuum energy density

A quantity more fundamental than the lagrangian is the action. For instance it is well-known that classical physics is based on a first principle, the least action principle, coupled with a relativity principle. Quantum effects can be seen as fluctuations of the action around its extremal value associated with the classical trajectory for particles or fields. Moreover the notion of scale transformation has to be formulated at the level of the action. The action is defined as the space-time integral of the lagrangian density. In case of QCD it reads :

$$S = \int d^4x \mathcal{L} = \int d^4x \left[ \bar{\psi} i \gamma^\mu (i \partial_\mu - t_a \bar{A}_{a\mu}) \psi - m \bar{\psi} \psi - \frac{1}{4g^2} \bar{G}_a^{\mu\nu} \bar{G}_{a\mu\nu} \right]. \quad (16)$$

To isolate the dependence of the coupling we have made the change of gluon variables  $\bar{A}_a^\mu = g A_a^\mu$  such that the gluon tensor  $\bar{G}$  defined by  $\bar{G}_a^{\mu\nu} = g G_a^{\mu\nu}$  does not have an explicit dependence on  $g$ . We limit our study to the light quark sector. We see that in the chiral limit ( $m = 0$ ) no explicit scale appears in the action. Hence the classical action is scale invariant and this invariance is only slightly broken by physical quark masses. The mathematical consequences of this quasi scale invariance can be studied by introducing an infinitesimal scale transformation

$$x \rightarrow (1 - \delta\lambda)x \quad \psi \rightarrow (1 + D_\psi \delta\lambda)\psi \quad \bar{A}_a^\mu \rightarrow (1 + D_A \delta\lambda)\bar{A}_a^\mu$$

where  $D_\psi = 3/2$  and  $D_A = 1$  are the dimensions (in unit of mass) of the fields. Let us calculate the variation of the action under the above dilatation transformations. Formally, one obtains the general result based on Noether theorem

$$\delta S = \int d^4x \delta\lambda \partial_\mu D_{dil}^\mu \quad \text{with} \quad \partial_\mu D_{dil}^\mu \equiv \partial_\mu (x_\nu T^{\nu\mu}) = T^\mu_\mu \quad (17)$$

where  $T^{\nu\mu}$  is the stress tensor of the system. The quantity  $D_{dil}^\mu$  is the dilatation current. If there is scale invariance the action should be invariant, which implies that the quadri-divergence of this current vanishes, *i.e.*, the dilatation current is conserved. We now calculate explicitly the variation of the action for the particular QCD lagrangian. The result is :

$$\delta S = \int d^4x \left[ \delta\lambda \sum_i (D_i - 4) \mathcal{L}_i + \delta\lambda \frac{\delta\mu}{\delta\lambda} \frac{1}{2g^3} \frac{dg}{d\mu} (\bar{G}_a^{\mu\nu} \bar{G}_{a\mu\nu}) \right]. \quad (18)$$



The first contribution to the the variation of the action is purely classical and depends on the field dimension  $D_i$  of the various pieces of the Lagrangian. We see that only the mass term ( $D = 3$ ) breaks scale invariance. The second contribution is associated with quantum fluctuations. In this qualitative approach, the action is seen as an effective action for the theory formulated at the scale  $a = 1/\mu$ . It is thus natural that the change of scale affects  $\mu$  as  $\mu \rightarrow (1 + \delta\lambda)\mu$ . Hence  $\delta g/\delta\lambda = (dg/d\mu)(\delta\mu/\delta\lambda) = \mu dg/d\mu = \beta(g)$  and the  $\beta$  function appears explicitly in the variation of the action. Identifying the two expressions (17) and (18) of  $\delta S$ , one obtains the trace anomaly relation [4] :

$$T^\mu_\mu = m\bar{\psi}\psi + \frac{\beta(g)}{2g^3} (g^2 G_a^{\mu\nu} G_{a\mu\nu}). \quad (19)$$

The second terms is anomalous in the sense that it is generated by quantum fluctuations and is absent at the classical level.

From Lorentz covariance we expect that the vacuum expectation value of the stress tensor is

$$\langle T^{\mu\nu} \rangle = \epsilon g^{\mu\nu}$$

and  $\epsilon$  is the energy density of the QCD vacuum. We know take the expectation value of the trace anomaly equation (19) on the QCD ground state. Ignoring the small quark mass term one obtains :

$$4\epsilon = 4\pi^2 \frac{\beta(g)}{2g^3} \left\langle \frac{g^2}{4\pi^2} G_a^{\mu\nu} G_{a\mu\nu} \right\rangle \quad (20)$$

In the above formula only non perturbative soft vacuum fluctuations are considered. The divergent sum of zero point oscillations up to infinite momentum has to be subtracted. From the general arguments given above (see eq. 13,14) we expect for sufficiently large scale,

$$\epsilon = C_\epsilon \mu^4 \exp\left(\frac{-4}{2\beta_0 g^2}\right) = C_\epsilon \Lambda_{QCD}^4, \quad (21)$$

which has to be understood as the energy density of the true QCD vacuum with respect to the perturbative vacuum. Of course it has to be negative. The expectation value  $\langle (\alpha_S/\pi) G_a^{\mu\nu} G_{a\mu\nu} \rangle$  with  $\alpha_S = g^2/4\pi$  is conventionally defined as the gluon condensate. It actually depends on the scale. It can be extracted phenomenologically from QCD sum rule analysis at scale around  $1\text{ GeV}$  [5]. The accepted value is  $\langle (\alpha_S/\pi) GG \rangle \simeq 0.012\text{ GeV}^4$ . Assuming that at this scale we can apply the leading order value for  $\beta(g)$ , we can get an estimate of the vacuum energy density :

$$\epsilon = -0.5\text{ GeV} \cdot fm^{-3}. \quad (22)$$

The physical meaning of this result is the following:  $|\epsilon|$  represents the energy which has to be furnished to expel non perturbative quantum fluctuations from a volume of one  $fm^3$ .

## 2.4 Qualitative picture of the nucleon

Lets us consider the nucleon in the MIT bag model picture [6]. It appears as a color singlet made of three free quarks moving in a spherical bubble of radius  $R$  of perturbative vacuum created by the confinement mechanism. The quark orbital wave function and energy correspond to the lowest cavity mode. They are obtained as a solution of a Dirac equation for a free quark with confining boundary conditions (infinite scalar potential in  $r = R$ ). Since  $R$  is the only scale the orbital energy should behave as  $e \approx 1/R$ . The explicit solution of the Dirac equation gives  $e = \Omega_0/R$  with  $\Omega_0 = 2.043$ . To get the full nucleon mass one has to add the energy needed to dig a hole of perturbative vacuum of volume  $V = (4\pi/3)R^3$  in the QCD ground state. This energy is  $E_V = BV$  where  $B$  is called the bag constant in the terminology used by the MIT group [6]. In principle it has to be identical with the absolute value,  $|\epsilon|$ , of the vacuum energy density. The quantity  $B$  also represents the pressure  $P = -\epsilon$  exerted by the QCD vacuum on the bubble. Hence in the simplest version of the MIT bag model the nucleon mass is :

$$M_N = \frac{3\Omega_0}{R} + \frac{4}{3}\pi R^3 B. \quad (23)$$

The equilibrium radius is obtained by minimization of the nucleon mass :

$$-\frac{dM_N}{dV} = \frac{3\Omega_0}{4\pi R^4} - B = 0 \Rightarrow R_h = \left(\frac{3\Omega_0}{4\pi}\right)^{1/4} \frac{1}{B^{1/4}} \simeq 1/\Lambda_{QCD} \simeq 1 \text{ fm}. \quad (24)$$

This is nothing but the mechanical equilibrium condition between the kinetic pressure exerted by the quarks and the vacuum pressure. To recover a nucleon radius around  $1 \text{ fm}$ , we must have  $B \simeq 0.1 \text{ GeV} \cdot \text{fm}^{-3}$  which is much smaller than the value  $|\epsilon| = 0.5 \text{ GeV} \cdot \text{fm}^{-3}$  deduced from the QCD sum rule. Although phenomenologically not so bad, it is important to realize that the bag model is only an effective realization of quark confinement, which must not be taken too literally. It is plausible that the non perturbative fluctuations are expelled from a much smaller volume [7]. Indeed lattice simulations strongly suggest that the true picture is a Y shaped color string or flux tube terminated by quarks. The length of these flux tubes are  $R_h \simeq 1/\Lambda_{QCD}$  and the quarks are probably constituent quark getting their mass,  $M_q \simeq 300 \text{ MeV}$ , from the chiral condensate. The size of these constituent quarks is presumably  $1/\Lambda_{\chi SB}$  where  $1/\Lambda_{\chi SB} \simeq 1 \text{ GeV}$  is a characteristic scale associated with a very important symmetry of QCD named chiral symmetry. This topic is the subject of the next section.

### 3 $SU(N_f)_L \otimes SU(N_f)_R$ chiral symmetry

This section is devoted to a very important global symmetry of QCD in the light quark sector, the  $SU(N_f)_L \otimes SU(N_f)_R$  chiral symmetry. The number  $N_f$  refers to the number of quark flavors which are involved. For  $N_f = 2$  only  $u$  and  $d$  quarks are considered, whereas  $N_f = 3$  includes the strange quark. The quality of the symmetry depends on the smallness of the quark masses as compared to typical hadron masses,  $M_H \sim 1 \text{ GeV}$ . This is clearly the case for  $N_f = 2$  involving only  $u$  and  $d$  quarks. In the following we will concentrate mainly on the  $N_f = 2$  symmetry but all what we will say can be applied to some extent to the strange quark sector ( $N_f = 3$ ) although the symmetry under discussion is less good since  $m_s \simeq 150 \text{ MeV}$ .

We introduce a column vector (isospinor) made of  $u$  and  $d$  quark fields and the associated line vector :

$$\psi = \begin{pmatrix} \psi_u \\ \psi_d \end{pmatrix}$$

$$\bar{\psi} = \psi^\dagger \gamma^0 = (\bar{\psi}_u, \bar{\psi}_d).$$

The QCD lagrangian (ignoring glue and quark colors which do not play any role for the symmetry consideration under discussion) can be straightforwardly re-expressed in terms of these objects :

$$\begin{aligned} \mathcal{L}_{QCD} &= i\bar{\psi}_u \gamma^\mu \partial_\mu \psi_u + i\bar{\psi}_d \gamma^\mu \partial_\mu \psi_d - m_u \bar{\psi}_u \psi_u - m_d \bar{\psi}_d \psi_d \\ &= i\bar{\psi} \gamma^\mu \partial_\mu \psi - \frac{m_u + m_d}{2} \bar{\psi} \psi - \frac{m_u - m_d}{2} \bar{\psi} \tau_3 \psi. \end{aligned} \quad (25)$$

We first notice that the lagrangian is invariant under the simple  $U(1)$  phase transformation  $\psi \rightarrow e^{i\alpha} \psi$ . The associated conserved Noether charge is  $Q = \int d\mathbf{r} \psi^\dagger \psi$  which is nothing but (three times) the baryon number. This symmetry (which can be extended to the heavy quark sector) is baryon number conservation. In the chiral limit (when quark masses exactly vanish) there is another  $U(1)$  axial symmetry associated with the transformation  $\psi \rightarrow e^{i\gamma_5 \alpha} \psi$ . This symmetry is actually broken by quantum loops : this is the so called axial anomaly. We will not discuss this point here although it is by itself a very important (and delicate) subject.

#### 3.1 Vector, axial and chiral symmetry

**Vector symmetry.** Let us consider the  $SU(2)$  vector transformation :

$$\psi \rightarrow e^{i\alpha_k \frac{\tau_k}{2}} \psi$$

where the  $\alpha_k$ 's ( $k = 1, 2, 3$ ) are real continuous parameters and the  $\tau_k$ 's are Pauli matrices acting on isospin indices. The only non invariant piece of the lagrangian (25) is the term proportional to  $m_u - m_d$  since it involves a  $\tau_3$  matrix. However this (isospin) violation is very small :  $(m_d - m_u)/2 \simeq 2 \text{ MeV} \ll M_H \sim 1 \text{ GeV}$ , and we will forget it most of the time. In this case QCD possesses an exact vector or isospin  $SU(2)$  symmetry. The associated Noether current is the vector current,  $\mathcal{V}_k^\mu$ , and the associated charges coincide with the three components,  $Q_k \equiv I_k$ , of the isospin operator :

$$\mathcal{V}_k^\mu = \bar{\psi} \gamma^\mu \frac{\tau_k}{2} \psi, \quad Q_k = \int d\mathbf{r} \psi^\dagger \frac{\tau_k}{2} \psi \equiv I_k. \quad (26)$$

In case of exact symmetry ( $m_u = m_d$ ) the current is conserved,  $\partial_\mu \mathcal{V}_k^\mu = 0$ , and the isospin  $Q_k$  is time independent. The isospin operators satisfy the  $SU(2)$  Lie algebra

$$[Q_i, Q_j] = i \epsilon_{ijk} Q_k$$

which is exactly the same as the angular momentum algebra associated with rotational symmetry. These operators are the generators of the  $SU(2)$  group and the quantum states transform as :

$$|\Phi\rangle \rightarrow |\Phi'\rangle = U |\Phi\rangle \quad \text{with} \quad U = e^{-i\alpha_j Q_j}. \quad (27)$$

From the QCD lagrangian, the hamiltonian  $H$  can be built. In the limit of exact symmetry ( $m_u = m_d$ ), the Hamiltonian operator commutes with the isospin operators ( $[Q_k, H] = 0$ ). This symmetry associated with the Lie algebra leads to a degenerate multiplet structure of the hadron spectrum analog to the multiplets originating from rotational symmetry in atoms :

$$|\alpha IM\rangle = \phi_{\alpha IM} |0\rangle \quad \text{with} \quad I = 0, \frac{1}{2}, 1, \dots, M = -I, -I+1, \dots, I. \quad (28)$$

The index  $\alpha$  represents all the other quantum numbers (spin, parity,...) needed to fully specify the hadron state and  $\phi_{\alpha IM}$  is some field operator acting on the QCD ground state and carrying the quantum numbers of the state under consideration. This multiplet structure is actually a well established experimental fact and well known examples are the doublet of  $J^\pi = (1/2)^+$  nucleons or the triplet of  $J^\pi = 0^-$  pions. In reality the degeneracy inside the multiplet is not exact. There is a small isospin splitting inside the multiplets of the order of  $1 \text{ MeV}$ , the main origin being the combined effect of the mass difference between the  $u$  and  $d$  quarks and the Coulomb interaction between quarks. In the case of the nucleon the neutron-proton mass difference,  $\Delta M_N = M_n - M_p$ , receives a contribution of  $\sim 2 \text{ MeV}$  from the quark mass difference and of  $\sim -1 \text{ MeV}$  from the Coulomb interaction. This multiplet structure can be extended to the strange sector. The hadrons can be classified according to the irreducible representations of the flavor  $SU(3)$  group: nucleon octet, pseudo-scalar octet, resonance decuplet, .. . The mass splitting inside the multiplets between strange and non strange hadrons is however much larger, of the order of  $100 - 200 \text{ MeV}$ .

It is important to realize that the very existence of the multiplet structure is related to the fact that the isospin of the vacuum is zero,  $Q_k |0\rangle = 0$ . The operator  $\phi_{\alpha IM}$  has to transform as the quantum state

$$U \phi_{\alpha IM} U^\dagger = \Sigma_{M'} \phi_{\alpha IM'} \langle \alpha IM' | U | \alpha IM \rangle \quad (29)$$

where  $\langle \alpha IM' | U | \alpha IM \rangle \equiv \mathcal{D}^{IM}$  is a rotation matrix element. It follows that :

$$\begin{aligned} U | \alpha IM \rangle &= U \phi_{\alpha IM} |0\rangle = U \phi_{\alpha IM} U^\dagger U |0\rangle \\ &= \Sigma_{M'} \phi_{\alpha IM'} U |0\rangle \langle \alpha IM' | U | \alpha IM \rangle \\ &= \Sigma_{M'} | \alpha IM' \rangle \langle \alpha IM' | U | \alpha IM \rangle. \end{aligned}$$

Hence by application of the “isospin rotation” operator  $U$  it is possible to generate the full multiplet. This is possible since :

$$U |0\rangle = |0\rangle \quad \Longleftrightarrow \quad Q_j |0\rangle = 0. \quad (30)$$

The multiplet structure is thus realized because the QCD ground state is invariant under an isospin transformation, *i.e.*, its isospin is zero.

**Axial symmetry.** We now consider an “axial” transformation which differs from the vector transformation by the presence of the odd  $\gamma_5$  matrix in the exponent :

$$\psi \rightarrow e^{i\alpha_k \frac{\tau_k}{2} \gamma_5} \psi. \quad (31)$$

The associated Noether current is the axial current which is of pseudo-vector nature, from which one can define the axial charges :

$$\mathcal{A}_k^\mu = \bar{\psi} \gamma^\mu \gamma_5 \frac{\tau_k}{2} \psi, \quad Q_k^5 = \int d\mathbf{r} \psi^\dagger \gamma_5 \frac{\tau_k}{2} \psi. \quad (32)$$

At variance with the vector case the pure mass term,  $(m_u + m_d) \bar{\psi} \psi$ , in the lagrangian is not conserved but the axial symmetry violation is very weak since  $m = (m_u + m_d)/2 \simeq 7 \text{ MeV} \ll M_H$ . The axial current is almost exactly conserved :

$$\partial_\mu \mathcal{A}_k^\mu = m i \bar{\psi} \gamma_5 \tau_k \psi. \quad (33)$$

To go further it is appropriate to reformulate the problem of vector and axial symmetries in a different way by introducing the concept of chiral symmetry.

**Chiral symmetry.** One introduces left handed and right handed quark fields :

$$\psi_L = \frac{1 - \gamma_5}{2} \psi, \quad \psi_R = \frac{1 + \gamma_5}{2} \psi. \quad (34)$$

The QCD Lagrangian can be rewritten in terms of left and right fields as :

$$\mathcal{L}_{QCD} = i \bar{\psi}_L \gamma^\mu \partial_\mu \psi_L + i \bar{\psi}_R \gamma^\mu \partial_\mu \psi_R - m (\bar{\psi}_L \psi_R + \bar{\psi}_R \psi_L). \quad (35)$$

The important feature brought by this new writing is the almost exact invariance of the lagrangian under  $SU(2)$  transformations acting separately on left and right handed quarks :

$$\begin{aligned} SU(2)_L : \quad \psi_L &\rightarrow e^{i\alpha_k \frac{\tau_k}{2}} \psi_L, & \psi_R &\rightarrow \psi_R \\ SU(2)_R : \quad \psi_R &\rightarrow e^{i\beta_k \frac{\tau_k}{2}} \psi_R, & \psi_L &\rightarrow \psi_L. \end{aligned} \quad (36)$$

One can accordingly define left and right charges

$$\begin{aligned} Q_L^k &= \int d\mathbf{r} \psi_L^\dagger \frac{\tau_k}{2} \psi_L = \frac{1}{2} (Q_k - Q_k^5) \\ Q_R^k &= \int d\mathbf{r} \psi_R^\dagger \frac{\tau_k}{2} \psi_R = \frac{1}{2} (Q_k + Q_k^5) \end{aligned} \quad (37)$$

which satisfy separate and independent  $SU(2)$  algebra :

$$[Q_R^i, Q_R^j] = i \epsilon_{ijk} Q_R^k, \quad [Q_L^i, Q_L^j] = i \epsilon_{ijk} Q_L^k, \quad [Q_R^i, Q_L^j] = 0. \quad (38)$$

### 3.2 Spontaneous breaking of chiral symmetry

The existence of the chiral symmetry seems to imply that two independent L and R worlds exist hence generating two identical sets of degenerate multiplets. In other words starting from an isospin multiplet with definite parity (this is always possible since parity commutes with  $H$  and isospin operators), one can generate a multiplet of degenerate chiral partners with opposite parity. Experimentally this is clearly not the case. For instance the first hypothetical chiral partner of the nucleon is a  $J^\pi = (1/2)^-$  resonance located around  $1.5 \text{ GeV}$ . Similarly the rho meson and the  $a_1$  meson which are candidate to be chiral partners have very different masses and spectral functions. As already mentioned the building up of a multiplet structure is actually related to the property of the vacuum under the symmetry. The multiplet structure arises only if the vacuum is invariant under the symmetry. This is the case for the vector transformation and one has :  $[H, Q_k] = 0$  and  $Q_k |0\rangle = 0$ . The symmetry is said to be realized *a la* Wigner.

Spontaneous breaking of chiral symmetry manifests in the fact that the vacuum is not invariant under an axial transformation or, said differently, the axial charge of the vacuum is not zero :  $Q_k^5 |0\rangle \neq 0$ . If we introduce the axial transformation acting on quantum states,

$$U = e^{-i\alpha_j Q_5} \quad |\Phi\rangle \rightarrow |\Phi'\rangle = U |\Phi\rangle, \quad (39)$$

one has  $U_5 |0\rangle \neq |0\rangle$ . It follows that there is no chiral partner multiplet :

$$\begin{aligned} U_5 |\alpha IM\rangle &= U_5 \phi_{\alpha IM} |0\rangle = U_5 \phi_{\alpha IM} U_5^\dagger U_5 |0\rangle \\ &= \Sigma_{M'} \phi_{\alpha IM'} U_5 |0\rangle = \langle \alpha IM' | U | \alpha IM \rangle \\ &\neq \Sigma_{M'} |\alpha IM'\rangle = \langle \alpha IM' | U | \alpha IM \rangle. \end{aligned}$$

The multiplet structure is not generated since the ground state is non invariant under the axial transformation.

**Summary of global symmetries in the light quark sector.** The original global symmetry at the classical level is actually  $U(2)_L \otimes U(2)_R$  and is broken to  $SU(2)_L \otimes SU(2)_R \otimes U(1)_V$  due to the  $U(1)_A$  anomaly and  $U(1)_V$  is associated with baryon number conservation. The  $SU(2)_L \otimes SU(2)_R$  chiral symmetry is spontaneously broken down to  $SU(2)_V$  according to the above discussion.

**Goldstone boson.** It remains nevertheless true that (in the chiral limit) the axial charge commutes with the hamiltonian. Its action on the vacuum should consequently give a state with the same energy. Let us introduce such a state :

$$|\pi_j\rangle = Q_j^5 |0\rangle.$$

Setting the ground state energy equal to zero for convenience, one has :

$$H |\pi_j\rangle = H Q_j^5 |0\rangle = Q_j^5 H |0\rangle = 0. \quad (40)$$

This implies the existence of soft (massless) modes which can be identified with the pions. Of course since there is an explicit breaking of chiral symmetry the physical pion is not exactly massless as we will see below.

**Basis of chiral perturbation theory.** Let us consider a state made of  $n$  such Goldstone modes with zero momenta. We have :

$$H |(\pi)^n\rangle = H (Q^5)^n |0\rangle = (Q^5)^n H |0\rangle = 0. \quad (41)$$

Hence the multipion state also has a zero energy. This implies that zero momentum massless pions do not interact. More generally low momentum physical pions only weakly interact. This is the basis of chiral perturbation theory.

**Order parameters.** We have already seen observational evidences in favor of spontaneous chiral symmetry breaking : the fact that there is no degenerate chiral partners and the existence of goldstone bosons, the pions. It is however also interesting to identify quantities, called order parameters, which characterize quantitatively the amount of chiral symmetry breaking. It turns out that the Noether currents associated with chiral symmetry are directly involved in the electroweak interaction. The  $W$  boson which is the agent of charged current weak interaction is coupled to the axial and vector hadronic currents. For instance the hadronic piece of the amplitude governing charged pion decay  $\pi^+ \rightarrow \mu^+ \nu_\mu$  is the matrix element of the axial current between the QCD ground state and the pion. The three pion states  $\pi^\pm, \pi^0$  constitute an isotriplet ( $I = 1$ ) and behave like an isovector. These eigenstates (spherical basis vectors) can be expressed in terms of cartesian states to make the writing more compact :

$$|\pi^\pm\rangle = \mp \frac{1}{\sqrt{2}} (|\pi_1\rangle \pm i |\pi_2\rangle), \quad |\pi^0\rangle = |\pi_3\rangle.$$

From translational invariance and covariance the matrix element of the axial current between a pion state and the vacuum is of the form

$$\langle 0 | \mathcal{A}_k^\mu(x) | \pi_j(p) \rangle = -i \delta_{jk} f_\pi p^\mu e^{-ipx} \quad (42)$$

where the constant  $f_\pi = 94 \text{ MeV}$ , which is called the pion decay constant, can be extracted from charged pion lifetime. The important point is that  $f_\pi$  is not zero. This is possible only if chiral symmetry is spontaneously broken as demonstrated below :

$$\langle 0 | Q_5^i(t) | \pi_j(\mathbf{q}) \rangle = \int d\mathbf{r} \langle 0 | \mathcal{A}_i^0(\mathbf{r}, t) | \pi_j(\mathbf{q}) \rangle = -\frac{i}{2} f_\pi e^{-im_\pi t} \langle \pi^i(0) | \pi^j(\mathbf{q}) \rangle. \quad (43)$$

If we take the particular case of zero momentum we see that  $f_\pi \neq 0 \Leftrightarrow Q_5^i | 0 \rangle \neq 0$ . Hence the pion decay constant,  $f_\pi = 94 \text{ MeV}$ , plays the role of an order parameter associated with the spontaneous breaking of axial symmetry.

It is possible to identify another order parameter by considering the operator identity :

$$[Q_5^i, [Q_j^5, H]] = \delta_{ij} \int d\mathbf{r} m \bar{\psi} \psi(\mathbf{r}). \quad (44)$$

We take the vacuum expectation values of both sides of the identity and insert a complete state of eigenstates of  $H$ ,  $|n\rangle$ , with eigenvalues  $E_n$  :

$$\sum_n 2E_n | \langle n | Q_5^i | 0 \rangle |^2 = - \int d\mathbf{r} 2m \langle \bar{q} q \rangle. \quad (45)$$

The above equation has the familiar form of an energy weighted sum rule in nuclear physics. If we saturate the sum rule with single pion states we obtain the celebrated Gell-Mann-Oakes-Renner (GOR) relation [8] :

$$m_\pi^2 f_\pi^2 = -2m \langle \bar{q} q \rangle \quad (46)$$

which is valid to lowest order in explicit breaking parameters  $m$  and  $m_\pi$ . In the rhs of the GOR relation it appears another order parameter which is the quark condensate :

$$\langle \bar{q} q \rangle = \frac{1}{2} \langle 0 | \bar{\psi}_u \psi_u + \bar{\psi}_d \psi_d | 0 \rangle = \frac{1}{2} \langle 0 | \bar{\psi}_L \psi_R + \bar{\psi}_R \psi_L | 0 \rangle. \quad (47)$$

Its non vanishing value explicitly demonstrates the existence of a mixing between left and right-handed quarks in the QCD vacuum. We note that the quantity  $\langle \bar{q} q \rangle$  is conventionally taken as being relative to one quark flavor. The rhs of the GOR relation involves parameters at the microscopic quark level associated with explicit ( $m$ ) and spontaneous ( $\langle \bar{q} q \rangle$ ) symmetry breaking. The interest of this relation is that these microscopic parameters are related to those appearing in the lhs which involves the macroscopic hadronic quantities associated with explicit ( $m_\pi$ ) and spontaneous ( $f_\pi$ ) symmetry breaking. If we take for the quark mass  $m = 6 \text{ MeV}$ , one obtains  $\langle \bar{q} q \rangle \simeq -(240 \text{ MeV})^3$ , which corresponds to a very large scalar density of quarks,  $-1.76 \text{ fm}^{-3} \simeq -10 \rho_0$ , in the QCD vacuum. This is the so called strong condensate scenario which seems to be confirmed by recent analysis. The gluon condensate discussed in the previous section and this quark condensate can be considered as the two very important numbers characterizing the QCD vacuum.

**The quark condensate.** The quark condensate is an example of order parameter. Such a quantity is not invariant under the symmetry group. Consequently it should vanish in the symmetric phase where the symmetry is restored in the Wigner mode. To elucidate this question we start with a familiar example from condensed matter physics.

Let us consider a spin system in the Heisenberg model for ferromagnet which is placed in an external magnetic field  $\vec{B}$ . The hamiltonian is :

$$H = -J \sum_{i,j} \vec{S}_i \cdot \vec{S}_j - \mu \sum_i \vec{S}_i \cdot \vec{B}. \quad (48)$$

In the absence of the external field this hamiltonian is obviously rotationally invariant. However under certain circumstances (temperature below the Curie point), the system may acquire a spontaneous magnetization :

$$\vec{M} = \frac{1}{N} \sum_i \vec{S}_i \neq 0. \quad (49)$$

The existence of such a definite direction breaks rotational symmetry. It is said that the symmetry is spontaneously broken. Of course rotating the magnetization would produce a state with the same energy and the ground state of the system is infinitely degenerate. The origin of the direction chosen by the system may come from random fluctuations. In presence of the external (even very small) magnetic field the direction of the magnetization is the one of the external magnetic field since the energy of the system will be lowered. The magnetization plays the role of an order parameter and vanishes beyond the Curie temperature where rotational symmetry is restored.

In the QCD case the Hamiltonian is :

$$H = H_0 + \int d^3r m (\bar{\psi}_L \psi_R + \bar{\psi}_R \psi_L) (\mathbf{r}). \quad (50)$$

What plays the role of the magnetization vector is the chiral condensate written in a matrix form in flavor space

$$M^{ij} = \langle 0 | \bar{\psi}_L^j \psi_R^i | 0 \rangle \quad (51)$$

where  $|0\rangle$  is the ground state with zero isospin and definite positive parity. If chiral symmetry is realized in the Wigner mode, left and right quarks live in two independent worlds and thus cannot mix in the QCD ground state. In that case the quark condensate vanishes identically. If chiral symmetry is spontaneously broken this is no longer the case. This quark condensate must have the following structure :

$$\langle 0 | \bar{\psi}_L^j \psi_R^i | 0 \rangle = \langle 0 | \bar{\psi}_R^j \psi_L^i | 0 \rangle = \frac{1}{2} \Sigma \delta^{ij} \neq 0. \quad (52)$$

The first equality comes from the parity invariance of the ground state and the second one from flavor invariance. The quantity  $\Sigma$  is the already introduced quark condensate also called chiral condensate. Indeed, the above formula can be reversed by taking the flavor trace :

$$\Sigma = \frac{1}{2} \langle 0 | \bar{\psi}_L \psi_R + \bar{\psi}_R \psi_L | 0 \rangle \equiv \frac{1}{2} \langle 0 | \bar{\psi}_u \psi_u + \bar{\psi}_d \psi_d | 0 \rangle \equiv \langle \bar{q}q \rangle. \quad (53)$$

Let us now make a chiral transformation  $U_L(\alpha)U_R(\beta)$  of the system. The ground state transforms as :

$$|0\rangle \rightarrow |\alpha, \beta\rangle = U_L(\alpha)U_R(\beta) |0\rangle. \quad (54)$$

We make use of the transformation law for the quark field :

$$U_L^\dagger(\alpha)\psi_L^i U_L(\alpha) = V_{ij}^\dagger(\alpha)\psi_L^j, \quad U_R^\dagger(\beta)\psi_R^i U_R(\beta) = V_{ij}^\dagger(\beta)\psi_R^j. \quad (55)$$

It follows immediately that the condensate matrix transform as :

$$M^{ij} \rightarrow M'^{ij} = \langle \alpha, \beta, \bar{\psi}_L^j \psi_R^i | \alpha, \beta \rangle = (V^\dagger(\beta) M V(\alpha))_{ij} = (V^\dagger(\beta) V^\dagger(\alpha))_{ij} \frac{\Sigma}{2}. \quad (56)$$

The pure vector (isospin) transformation is obtained with  $\alpha = \beta$ . In such a case the ground state (of zero isospin) is invariant and the condensate is also invariant. The pure axial transformation is obtained for  $\alpha = -\beta$ . In this case one has

$$M = \frac{\Sigma}{2} \rightarrow \frac{\Sigma}{2} (\cos\alpha + i\vec{\tau} \cdot \hat{\alpha} \sin\alpha)$$

where the angle  $\alpha$  is the norm of the vector  $\vec{\alpha} = (\alpha_1, \alpha_2, \alpha_3)$ . We see that the condensate has rotated in a four dimensional space as the magnetization did in ordinary space. The corresponding chirally rotated state is degenerate with the original state (taken conventionally with zero isospin and positive parity) but the condensate points in a direction characterized by the vector  $\vec{\alpha}$  which is the analog of the direction of

the magnetization in the ferromagnetic case. In the presence of explicit symmetry breaking, the quark mass appearing in the QCD hamiltonian plays the role of the external magnetic field. In such a case the orientation of the condensate is fixed by the way that chiral symmetry is explicitly broken: this corresponds to  $\alpha = 0$  which gives the lowest possible energy since  $\Sigma$  is negative.

All what was said concern the vacuum structure. However in presence of baryons (non vanishing density) or in presence of thermal excitations (non vanishing temperature) the situation will change. Indeed it is expected that at a certain temperature chiral symmetry will be restored. This subject is at the origin of an intense theoretical and experimental activities devoted to the phase structure of QCD, the major experimental tool being relativistic heavy ion collision. We will address these questions in the subsection 4.4 and in the last section.

**Correlators and spectral functions.** Details on the structure of a system can be systematically studied by looking at correlators. More precisely we will study correlations functions between currents or fields carrying the quantum numbers characteristic of a given hadron, taken at two different space-time point. Usually one studies these correlation functions in energy momentum space. One defines a current-current correlation function between two currents or fields having the quantum number of a given hadron :

$$\Pi_R(q) \equiv \Pi_R(q_0, \vec{q}) = -i \int d^4x e^{iq \cdot x} \Theta(x_0) \langle 0 | [J(x), J(0)] | 0 \rangle. \quad (57)$$

The analytical structure of the correlator allows to express it in a dispersive form

$$\Pi_R(q_0, \vec{q}) = \int_{-\infty}^{+\infty} d\omega \frac{S(\omega, \vec{q})}{q_0 - \omega + i\eta}$$

and all the properties of the hadron are encoded in the spectral function :

$$S(\omega, \vec{q}) = -\frac{1}{\pi} \text{Im} \Pi_R(\omega, \vec{q}) = \sum_f |\langle f | J(0) | 0 \rangle|^2 (2\pi)^3 \delta^{(3)}(\vec{q} - \vec{p}_f) \delta(\omega + E_0 - E_f). \quad (58)$$

This can be generalized at finite temperature  $T = 1/\beta$  for a systems described by a canonical ensemble :

$$S(\omega, \vec{q}) = -\frac{1}{\pi} \text{Im} \Pi_R(\omega, \vec{q}) = \sum_{i,f} \frac{e^{-\beta E_i}}{Z} (1 - e^{-\beta \omega}) |\langle f | J(0) | i \rangle|^2 (2\pi)^3 \delta^{(3)}(\vec{q} + \vec{p}_i - \vec{p}_f) \delta(\omega + E_i - E_f). \quad (59)$$

In the vacuum we get the well-known spectra with peaks for stable particles and bump for resonances. The chiral asymmetry of the vacuum is directly visible since there is no degeneracy between possible chiral partners transforming into each other under a chiral transformation. This translates into possibly very different spectral functions for chiral partners. A particularly spectacular example is provided by the vector and axial currents which encode the properties of the rho and  $a_1$  mesons. As shown on the left panel of fig. 2 the low parts of the spectra are very different but at higher energy where perturbative QCD (or more precisely quark-hadron duality) works they become identical. Hence spontaneous chiral symmetry breaking can be viewed as a low energy non perturbative phenomenon. One reason is that high momentum quarks involved in the high energy configurations decouple from the quark condensate. This point will be rediscussed later.

### 3.3 Explicit realization : the Nambu-Jona-Lasinio model

Although chiral symmetry breaking and restoration can be studied on the lattice the physical mechanisms at the QCD level and the relation to confinement is not yet really understood. It is one reason which makes useful to complement this approach by studying this problem with models. Among them a very popular one is the Nambu-Jona-Lasinio (NJL) model (see [10] or [11] for reviews) whose lagrangian in its simplest form is :

$$\mathcal{L}_{NJL} = i\bar{\psi}\gamma^\mu \partial_\mu \psi - m\bar{\psi}\psi + \frac{G_1}{2} \left[ (\bar{\psi}\psi)^2 + (i\bar{\psi}\gamma^5 \vec{\tau}\psi)^2 \right]. \quad (60)$$



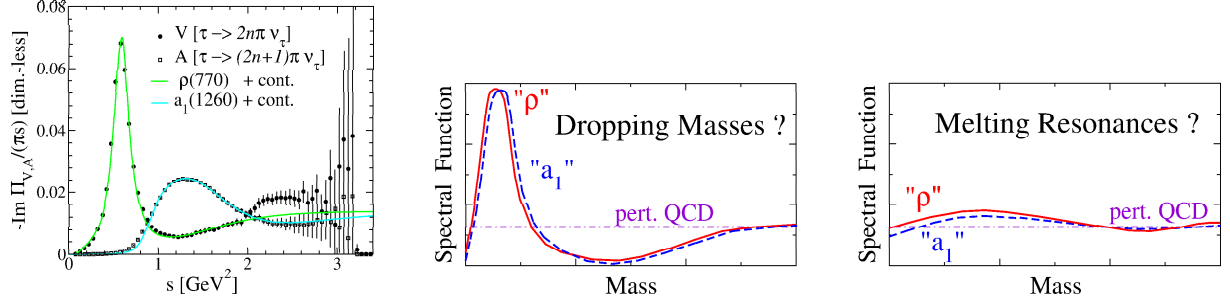


Figure 2: *Left panel: vector and axial vector spectral functions as measured in hadronic  $\tau$  decays [9]. Middle and right panels: scenarios for the effect of chiral restoration on the in-medium vector- and axial-vector spectral functions.*

There is a free piece with a current quark mass of a few MeV and a quartic chiral invariant contact interaction which is supposed to represent all the complicated interacting multi-gluons exchange. There are three parameters : the current quark mass  $m$  but essentially fixed to reproduce the pion mass, the strength  $G_1$  of the attractive interaction and a cutoff  $\Lambda$  in momentum space of the order of  $1\text{ GeV}$ . This cutoff will regularize divergent integrals but has a physical meaning. Only low momentum quarks below the cutoff strongly interact, the high momentum quarks, leaving in the world with asymptotic freedom, just decouple. If the coupling constant is sufficiently large the quark gets a finite constituent quark mass  $M$  which is the solution of the gap equation and this is associated with the building-up of a quark condensate. In the mean field approximation one makes the replacement

$$(\bar{\psi}\psi)^2 \simeq 2(\bar{\psi}\psi) \langle\langle \bar{\psi}\psi \rangle\rangle = 4(\bar{\psi}\psi) \langle\langle \bar{q}q \rangle\rangle.$$

and the gap equation reads :

$$\begin{aligned} M &= m - 2G_1 \langle\langle \bar{q}q \rangle\rangle \\ &= m + 4N_c G_1 \int_{p<\Lambda} \frac{d\mathbf{p}}{(2\pi)^3} \frac{M}{E_p} \end{aligned} \quad (61)$$

where  $E_p = \sqrt{p^2 + M^2}$  is the energy of the quasi-particle constituent quark.

It is an easy task to construct from the really empty bare vacuum  $|\phi_0\rangle$  the physical vacuum ground state,  $|\phi(M)\rangle$ , which is of BCS type showing that the large scalar quark density corresponds to a vacuum made of interacting quark-antiquark pairs :

$$\begin{aligned} |\phi(M)\rangle &= C \exp \left( - \sum_{s, p<\Lambda} \gamma_{ps} b_{\mathbf{p}s}^\dagger d_{-\mathbf{p}-s}^\dagger \right) |\phi_0\rangle \\ &= \prod_{s, p<\Lambda} \left( \alpha_p + s\beta_p b_{\mathbf{p}s}^\dagger d_{-\mathbf{p}-s}^\dagger \right) |\phi_0\rangle \end{aligned} \quad (62)$$

with

$$\begin{pmatrix} \alpha_p \\ \beta_p \end{pmatrix} = \left[ \frac{1}{2} \left( 1 \pm \frac{p^2 + Mm}{\epsilon_p E_p} \right) \right]^{\frac{1}{2}}, \quad \gamma_{ps} = -s\beta_p/\alpha_p.$$

The operators  $b_{\mathbf{p}s}^\dagger$  and  $d_{\mathbf{p}s}^\dagger$  are creation operators for a quark or antiquark with momentum  $\mathbf{p}$  and spin state  $s$ .

**Mesons, Goldstone theorem.** The mesons can be generated as collective  $q\bar{q}$  states in a formalism which is equivalent to the RPA in the many-body problem. One way is to build the unitarized  $q\bar{q}$  interaction in the various channels and from its pole structure one can extract the mass and the coupling

constant of the mesons. The quark-meson coupling constant,  $g$ , emerging in the calculation is such that :

$$g^2 = \frac{1}{2N_c N_f I_2(M)} \quad \text{with} \quad I_2(M) = \int_0^\Lambda \frac{d^3 k}{(2\pi)^3} \frac{1}{4 E_k^3}.$$

The pion decay constant is found to be  $f_\pi = M/g$ , which is nothing but the celebrated Goldberger-Treiman relation formulated at the quark level. The pion mass is :

$$m_\pi^2 = \frac{m g}{G_1 f_\pi} = \frac{m M}{G_1 f_\pi^2}. \quad (63)$$

In the chiral limit it exactly vanishes in agreement with Goldstone theorem. The second form, once combined with the gap equation allows to recover the GOR relation. Finally a scalar mode (sigma meson) shows up with mass  $m_\sigma^2 = 4M^2 + m_\pi^2$ . Hence one recovers the pion as a quasi Goldstone boson and the pion decay constant can be also obtained. The sigma mass is essentially twice the constituent mass. Using the above relations one can adjust the set of parameters to three quantities, the pion mass, the pion decay constant and the quark condensate. The value of the constituent quark mass is typically  $M \approx 350 \text{ MeV}$  in agreement with lattice estimate.

**Effective potential.** It is also very useful to formulate directly the model in terms of the physical hadrons. This can be done using path integral techniques starting from a kind of partition function, the so-called vacuum persistence amplitude. The idea is to insert in the functional integral a change of variables introducing scalar and pseudo-scalar boson fields and integrate over the fluctuating quark quantum field, in other words to integrate out quarks in the Dirac sea and project them on the mesonic degrees of freedom

$$\begin{aligned} Z &= \int d\psi d\bar{\psi} d\varphi_0 d\vec{\varphi} \delta(\varphi_0 - \bar{\psi}\psi) \delta(\vec{\varphi} - \bar{\psi}\gamma^5 \vec{\tau}\psi) \exp \left[ i \int d^4 x \mathcal{L}_{NJL}(\psi, \bar{\psi}) \right] \\ &= \int d\Sigma d\vec{\Pi} \int d\psi d\bar{\psi} d\varphi_0 d\vec{\varphi} \exp \left[ i \int d^4 x \left( \mathcal{L}_{NJL} + \Sigma(\varphi_0 - \bar{\psi}\psi) + \vec{\Pi} \cdot (\vec{\varphi} - \bar{\psi}\gamma^5 \vec{\tau}\psi) \right) \right] \\ &= \int d\Sigma d\vec{\Pi} \int d\psi d\bar{\psi} \exp \left[ i \int d^4 x \left( \bar{\psi} D\psi - \frac{\Sigma^2 + \vec{\Pi}^2}{2G_1} \right) \right] \\ &\approx \int d\Sigma d\vec{\Pi} \exp \left[ i \int d^4 x \mathcal{L}_{eff}(\Sigma, \vec{\Pi}) \right] \end{aligned} \quad (64)$$

where the Dirac operator is  $D(\Sigma, \vec{\Pi}) = i\gamma^\mu \partial_\mu - m - \Sigma - i\vec{\tau} \cdot \vec{\Pi} \gamma_5$ . The explicit integration over the quark field yields a highly non local lagrangian (the fermion determinant) which can be calculated as a loop or derivative expansion. To one loop one finds

$$\begin{aligned} \mathcal{L}_{eff}(\Sigma, \vec{\Pi}) &= \frac{1}{g^2} \left( \partial^\mu \Sigma \partial_\mu \Sigma + \partial^\mu \vec{\Pi} \cdot \partial_\mu \vec{\Pi} \right) - W(\Sigma, \vec{\Pi}) \\ W(\Sigma, \vec{\Pi}) &= \frac{\Sigma^2 + \vec{\Pi}^2}{2G_1} - 2N_c N_f \int_0^\Lambda \frac{d^3 k}{(2\pi)^3} \sqrt{k^2 + (\Sigma + m)^2 + \vec{\Pi}^2} \end{aligned} \quad (65)$$

where  $W(\Sigma, \vec{\Pi})$  is the chiral effective potential. After introduction of canonical fields defined by  $\sigma = (m + \Sigma)/g$  and  $\vec{\pi} = \vec{\Pi}/g$ , it can be well approximated by a linear sigma model potential :

$$W^{l\sigma m} = \frac{m_\sigma^2 - m_\pi^2}{8f_\pi^2} \left( \sigma^2 + \vec{\pi}^2 - \frac{m_\sigma^2 - 3m_\pi^2}{m_\sigma^2 - m_\pi^2} \right)^2 - f_\pi m_\pi^2 \sigma. \quad (66)$$

This effective potential has a Mexican hat shape, as depicted on fig. 3, typical of a spontaneous breaking of the chiral symmetry. It contains the energy of the Dirac sea of constituent quarks with mass  $M = g \langle \sigma \rangle \equiv g f_\pi$ . In the chiral limit ( $m = m_\pi = 0$ ) the degenerate vacua correspond to the chiral circle (shown on the right panel of fig. 3) at the bottom of the effective potential. Its equation is  $\sigma^2 + \vec{\pi}^2 = f_\pi^2$  and

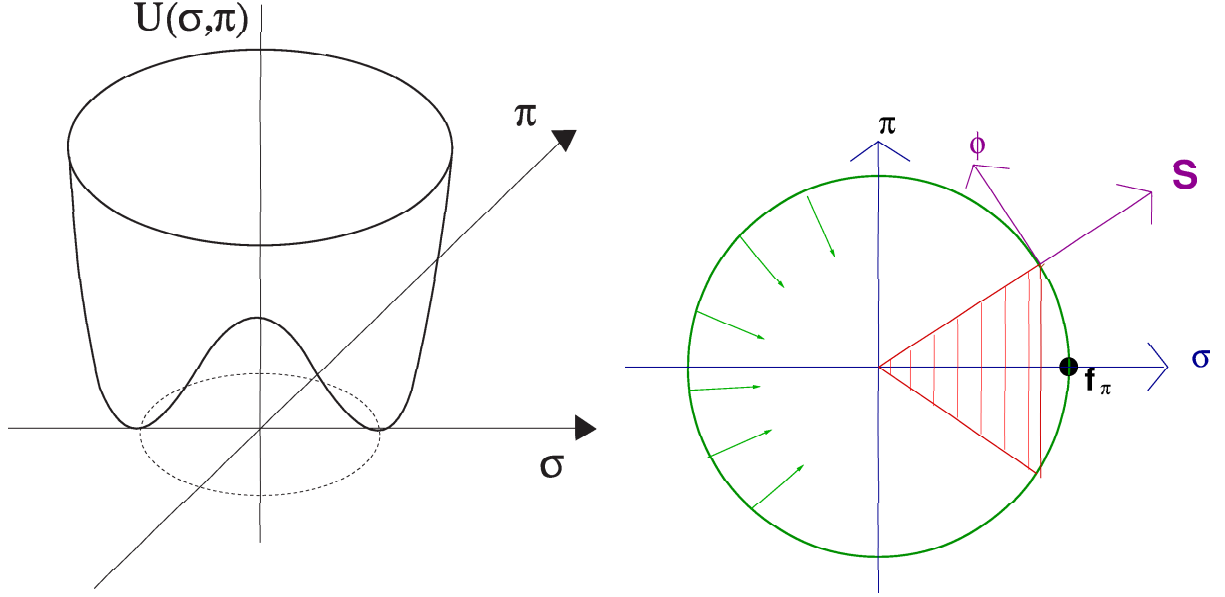


Figure 3: The “Mexican hat” chiral effective potential (left) and the chiral circle (right) .

the pseudo-scalar field (pion) lives on this circle and represents the phase fluctuation of the condensate. This pionic mode is massless since it does not cost energy to move on the chiral circle. The massive scalar mode represents the amplitude fluctuation of the condensate. These mesons can be also coupled to classical quark fields which can be identified with valence quarks for building models of the nucleon. It is also possible to generalize the model to incorporate vector mesons ( $\rho, \omega$ ) and axial-vector mesons ( $a_1$ ).

### 3.4 Chiral symmetry restoration

**Lattice results.** When hadronic matter is heated or compressed initially confined quarks and gluons start to percolate to be finally liberated. This picture is supported by lattice simulation at finite temperature showing that strongly interacting matter exhibits a sudden change in thermodynamic quantities, (possibly constituting a true phase transition) within a narrow temperature window around  $T_c = 180 - 190 \text{ MeV}$  [12]. On fig. 4 we see near the critical temperature a very rapid growing of the energy density (and other thermodynamical quantities such as pressure or entropy), signaling the transition from a hadronic resonance gas to the matter of deconfined quarks and gluons. This rapid rise of the energy density is usually interpreted to be due to the deconfinement, *i.e.*, associated with the liberation of many new degrees of freedom. This transition is accompanied by a dropping of the chiral condensate (see right panel of fig. 4) indicating chiral symmetry restoration. The critical temperature for chiral restoration is usually defined as the maximum of the chiral susceptibility  $\chi_m = \partial \langle \bar{q}q \rangle / \partial m$ . However why these two transitions seem to occur simultaneously is still an open question. There is also the domain of finite density and low temperature where lattice simulations are not easily feasible; here we have to rely on models and effective theories.

**Partial restoration of chiral symmetry.** We first recall the well known Feynman-Hellmann theorem. We consider a hamiltonian of the form  $H = H_0 + H'$  where  $H'$  linearly depends on a parameter  $\lambda$  according to  $H' = \lambda h'$ . Let us call  $|\Phi(\lambda)\rangle$  an exact normalized eigenstate of  $H$  with eigen-energy  $E(\lambda)$ . The theorem states that

$$\langle \Phi(\lambda) | H' | \Phi(\lambda) \rangle = \lambda \frac{\partial E(\lambda)}{\partial \lambda} \quad (67)$$

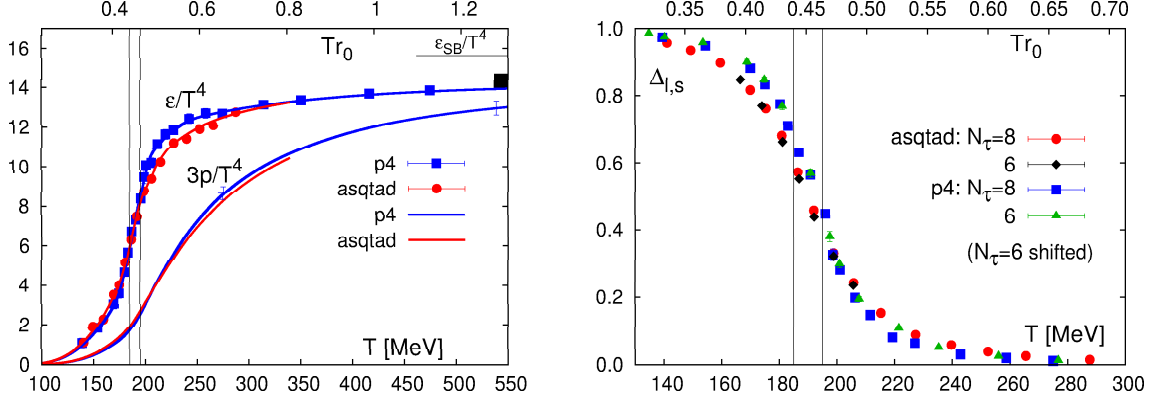


Figure 4: Lattice results [12] for energy density and pressure (left panel) and chiral condensate normalized to the zero temperature result (right panel).

We apply the theorem to the QCD case

$$H = H_0 + H_{\chi SB} = H_0 + m \int d\mathbf{r} \bar{\psi} \psi \quad (68)$$

where  $H_0$  is the full QCD hamiltonian in the chiral limit and  $m$  plays the role of  $\lambda$ .

As discussed just before chiral symmetry restoration is expected to be fully restored at finite temperature but also at finite density. However far before the full restoration the quark condensate starts to decrease through the simple presence of hadrons since the hadrons have a positive quark scalar density which partially compensates the negative scalar density of the vacuum. In a dilute medium each hadron present with scalar density  $\rho_{sh}$  contributes additively to the dropping of the quark condensate

$$\langle \bar{q}q \rangle = \langle \bar{q}q \rangle_{vac} + \sum_h \rho_{sh} Q_S^h \quad (69)$$

where  $Q_S^h = \int d^3r \langle \bar{q}q(\vec{r}) \rangle_h$  is the scalar charge of the hadron  $h$ . We can also introduce the hadron sigma term defined as the expectation value on the hadron state of a double commutator involving the axial charge which is identically equal to the chiral symmetry breaking piece of the hamiltonian:

$$\sigma_h = \langle h [Q_i^5, [Q_i^5, H]] | h \rangle_{conn} = \langle h | H_{\chi SB} | h \rangle \equiv \int d\mathbf{r} m \langle h | \bar{\psi} \psi(\mathbf{r}) | h \rangle \equiv 2m Q_S^h = m \frac{\partial M_h}{\partial m} \quad (70)$$

It is implicit in the previous matrix elements that the vacuum contribution has been subtracted and one reconstitutes the scalar charge of the hadron. The last equality comes from the Feynman-Hellman theorem since  $H_{\chi SB}$  is linear in  $m$ . The result given in eq. (69) is valid for dilute non interacting matter but a more general result can be obtained since the quark condensate can be obtained directly from the equation of state. For this purpose we consider the grand potential in the grand canonical ensemble at temperature  $T$  and baryonic chemical potential  $\mu_B$ :

$$\Omega(V, T, \mu_B) = -T \ln Z = -T \ln \left( \text{Tr} \left[ e^{-(H_{QCD} - \mu_B N_B)} \right] \right) = \Omega_{vac} - V P(T, \mu_B) \equiv V \omega(T, \mu_B) \quad (71)$$

Thanks to the Feynman-Hellmann theorem the quark condensate can be obtained by taking the derivative of the grand potential with respect to the quark mass:

$$\langle \langle \bar{q}q \rangle \rangle (T, \mu_B) = \frac{1}{2} \left( \frac{\partial \omega}{\partial m} \right)_{\mu_B} = \langle \bar{q}q \rangle_{vac} - \frac{1}{2} \left( \frac{\partial P}{\partial m} \right)_{\mu_B}. \quad (72)$$

Hence the evolution of the quark condensate is exactly known once the pressure  $P(T, \mu_B, m)$  is known.

**Chiral restoration and hadron structure** Using the GOR relation (46) the evolution of the quark condensate in the dilute approximation (eq. 69) can be rewritten as :

$$\frac{\langle \bar{q}q \rangle}{\langle \bar{q}q \rangle_{vac}} = 1 - \sum_h \frac{\rho_{sh} \sigma_h}{f_\pi^2 m_\pi^2}. \quad (73)$$

We see that each hadron present in a medium with a (scalar) density  $\rho_{sh}$  contributes to the evolution of the condensate by an amount governed by its sigma term. Its dropping depends a priori on all the present species of hadrons. Fortunately only the lightest hadrons contribute since heavy hadrons just decouple from the condensate. This is simply because in heavy hadrons the mass of the quarks having large momenta drops according to lattice [13] and instanton model [14] results. In other words the higher states in the spectrum are not sensitive to the chiral asymmetry of the vacuum and it is plausible that each baryon recovers a degenerate chiral partner with opposite parities [15]. This feature has to be connected with the convergence of spectral functions of chiral partners at large energy. To leading order in density and temperature one gets an approximate but model independent result :

$$\frac{\langle \bar{q}q \rangle}{\langle \bar{q}q \rangle_{vac}} \approx 1 - 0.35 \frac{\rho}{\rho_0} - \frac{T^2}{8f_\pi^2}. \quad (74)$$

The first term corresponds to the contribution of the nucleons calculated with a sigma term  $\sigma_N \simeq 50 \text{ MeV}$  showing that in ordinary cold nuclear matter one already has more that thirty percent dropping of the condensate. Notice that we have replaced the scalar density by the ordinary one since at low density the nucleons are non relativistic and there is no difference between these two densities. The second term comes from the thermal medium approximated by a non interacting massless pion gas; this result corresponds to the leading term in chiral perturbation theory. From the above discussion it is clear that there is an interplay between chiral restoration and hadron structure since the dropping of the condensate is driven by the values of the sigma terms. These sigma terms which are related to the masses are intrinsic properties of the hadrons and depend on their structure and in particular on the respective roles of chiral symmetry breaking and quark confinement mechanism in the generation of the mass [16]. The sigma term of the nucleon, also called the pion-nucleon sigma term, can be obtained by a non straightforward analysis of pion-nucleon data. The accepted value is around  $50 \text{ MeV}$ . It can be also extracted from lattice data but some extrapolation of the data to the physical quark mass is needed using either chiral perturbation theory [17] or a chiral model of the nucleon [18]. One advantage of the model analysis is to demonstrate that the virtual pion cloud surrounding the quark core is responsible from almost half of the pion-nucleon sigma term.

**Fluctuations of the chiral condensate and chiral susceptibilities.** When approaching a phase transition it is always important to study fluctuations, in particular the ones related to order parameters. In magnetism the magnetic susceptibility is  $\chi_m = \partial M / \partial B$ . It represents the modification of the magnetization induced by a small external magnetic field. Having in mind the analogy with the Heisenberg ferromagnet seen in subsection 3.2, the exact analog in the QCD case is the scalar susceptibility,  $\chi_S = \partial \langle \bar{q}q \rangle / \partial m$ , representing the modification of the quark condensate in presence of the small quark mass. Using linear response theory it is related to the correlator,  $G_S(\mathbf{r}, t, \mathbf{r}', t')$ , of the scalar quark density fluctuations taken at zero energy and momentum going to zero :

$$\chi_S = \frac{\partial \langle \bar{q}q \rangle}{\partial m} = 2 \int dt' d\mathbf{r}' \Theta(-t') \langle -i [\delta \bar{q} q(0), \delta \bar{q} q(\mathbf{r}', t')] \rangle = 2 \text{Re} G_S(\omega = 0, \vec{q} \rightarrow 0). \quad (75)$$

In the spirit of what was said previously it is interesting to compare the susceptibility associated with chiral partners : the scalar one,  $\chi_S$ , which encodes the property of the sigma meson and the pseudo-scalar one,  $\chi_{PS}$ , which encodes the properties of the pion.  $\chi_{PS}$  involves the pseudo-scalar pion-like operator  $\bar{q} i\gamma_5 \frac{\tau_\alpha}{2} q$  which can be generated from the scalar operator,  $\bar{q}q$ , by an axial transformation, hence these two operators are chiral partners. This pseudo-scalar susceptibility is defined from the pseudo-scalar correlator and describes the propagation of pion-like excitations :

$$\chi_{PS} = 2 \int dt' d\mathbf{r}' \Theta(-t') \langle -i \left[ \bar{q} i\gamma_5 \frac{\tau_\alpha}{2} q(0), \bar{q} i\gamma_5 \frac{\tau_\alpha}{2} q(\mathbf{r}', t') \right] \rangle = \frac{\langle \bar{q}q \rangle(\rho)}{m}. \quad (76)$$

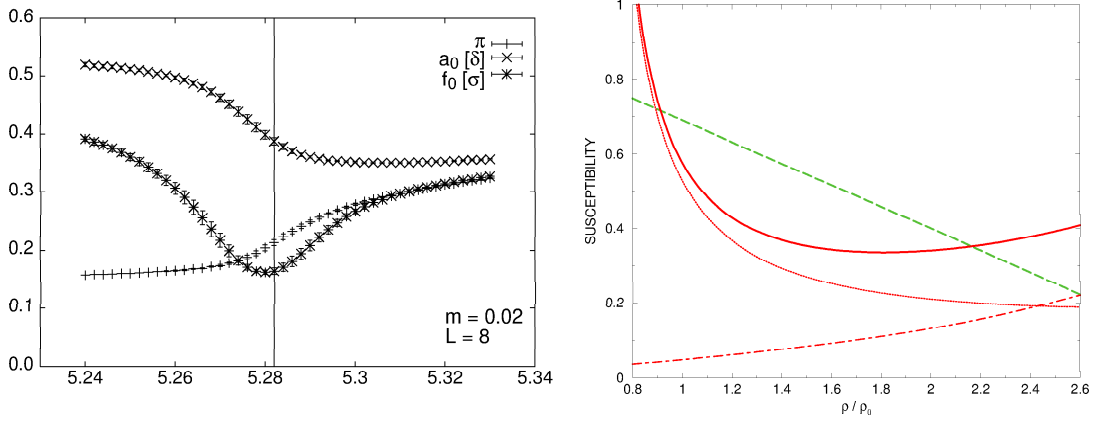


Figure 5: *Left panel: square root of the inverse of the scalar ( $\sigma$ ) and pseudo-scalar ( $\pi$ ) thermal susceptibilities versus lattice units representing temperature from [21]. Right panel: Density evolution of the pseudoscalar susceptibility (dashed curve) and of the scalar susceptibility (full curve) with its pionic contribution (dot-dashed curve) and its p-h contribution (dotted curve) [22].*

The second equality shows that it is related to the quark condensate, using partially conserved axial current (eq. 33) and soft pions theorems [19]. The scalar susceptibility can be calculated in various ways : from the equation of state, using a model or using a dispersive approach :

$$\chi_S = \frac{1}{2} \left( \frac{\partial^2 \omega}{\partial m_q^2} \right)_\mu = 2 \operatorname{Re} G_S(\omega = 0, \vec{q} \rightarrow 0) = \int_0^\infty d\omega \left( -\frac{2}{\pi\omega} \right) \operatorname{Im} G_S(\omega, \vec{q} = 0). \quad (77)$$

The last equality involves the integral of the scalar spectral function which is expected to receive an important contribution of low-lying nuclear excitations at finite density [20].

The thermal scalar susceptibility can be calculated on the lattice [21] as shown on the left panel of fig. 5. It becomes very large near the phase transition as expected for a second order or weak first order transition. What is actually plotted on fig. 5 is (the square root of) the inverse of the scalar and pionic susceptibilities versus some lattice units representing temperature. At low temperature they are very different (they essentially scale like the sigma and pion masses). Near the phase transition the scalar one becomes very large showing that the sigma becomes a soft mode. At high temperature they become identical and this is a genuine signature of chiral restoration. Unfortunately the finite density, low  $T$  susceptibilities are not available on the lattice but it is possible to get an estimate using an effective chiral theory. For example in the linear sigma model-based approach one makes the replacement :

$$\bar{q}q \rightarrow \frac{\langle \bar{q}q \rangle_{vac}}{f_\pi} \sigma.$$

In this approach the in-medium scalar quarks density fluctuations are transmitted by the sigma meson and are relayed by p-h excitations dressing it. We also see a convergence effect accelerated by the pion cloud contribution which might be attributed to chiral restoration although it is still an open question [22].

**Correlator mixing.** Let us come back to the vector and axial-vector currents :

$$\mathcal{V}_k^\mu = \bar{\psi} \gamma^\mu \frac{\tau_k}{2} \psi, \quad \mathcal{A}_k^\mu = \bar{\psi} \gamma^\mu \gamma_5 \frac{\tau_k}{2} \psi. \quad (78)$$

The properties of these currents in the medium are encoded in the vector and axial-vector correlators :

$$\Pi_V^{\mu\nu}(q) = -i \int d^4x e^{iq \cdot x} \langle\langle \mathcal{T}(\mathcal{V}_k^\mu(x), \mathcal{V}_k^\nu(0)) \rangle\rangle \quad (79)$$

$$\Pi_A^{\mu\nu}(q) = -i \int d^4x e^{iq \cdot x} \langle\langle \mathcal{T}(\mathcal{A}_k^\mu(x), \mathcal{A}_k^\nu(0)) \rangle\rangle. \quad (80)$$

In the vacuum their imaginary part are determined by the vector and axial spectral densities,  $\rho_V(q^2)$  and  $\rho_A(q^2)$  which are the quantities containing the physical information. From Lorentz covariance and current conservation they must have the form :

$$-\frac{1}{\pi} \text{Im} \Pi_V^{\mu\nu}(q; T=0) = -(q^2 g^{\mu\nu} - q^\mu q^\nu) \rho_V(q^2) \quad (81)$$

$$-\frac{1}{\pi} \text{Im} \Pi_A^{\mu\nu}(q; T=0) = q^\mu q^\nu f_\pi^2 \delta(q^2 - m_\pi^2) - (q^2 g^{\mu\nu} - q^\mu q^\nu) \rho_A(q^2). \quad (82)$$

The first term in the axial correlator corresponds to the pion component,  $f_\pi \partial^\mu \phi$ , of the axial current and the spectral densities  $\rho_V$  and  $\rho_A$  are saturated by  $\rho$  and  $a_1$  mesons as shown on the left panel of fig. 2. Experimentally they have been obtained simultaneously by the ALEPH collaboration at LEP from the hadronic decays of the tau lepton in even or odd number of pions [9, 23].

From chiral symmetry alone it is possible to show that, to order  $T^2$  in the chiral limit, the only medium effect is the mixing of the two correlators without any mass shift [24] :

$$\Pi_V^{\mu\nu}(q; T) = (1 - \epsilon) \Pi_V^{\mu\nu}(q; T=0) + \epsilon \Pi_A^{\mu\nu}(q; T=0) \quad (83)$$

$$\Pi_A^{\mu\nu}(q; T) = (1 - \epsilon) \Pi_A^{\mu\nu}(q; T=0) + \epsilon \Pi_V^{\mu\nu}(q; T=0). \quad (84)$$

At this order there is no dropping rho mass. The mixing parameter  $\epsilon$  is related to the pion scalar density  $\langle\langle \Phi^2 \rangle\rangle$  in a thermal bath with pion occupation number  $n_k = (\exp(\beta k) - 1)^{-1}$  :

$$\epsilon = \frac{2}{3} \frac{\langle\langle \Phi^2 \rangle\rangle}{f_\pi^2} = \frac{2}{f_\pi^2} \int \frac{d\mathbf{k}}{(2\pi)^3} \frac{n(\omega_k)}{\omega_k} = \frac{T^2}{6 f_\pi^2}. \quad (85)$$

It also follows that the pion decay constant drops according to

$$\frac{f_\pi^*(T)}{f_\pi} = \sqrt{1 - \epsilon} \simeq 1 - \frac{1}{3} \frac{\langle\langle \Phi^2 \rangle\rangle}{f_\pi^2} = 1 - \frac{T^2}{12 f_\pi^2} \quad (86)$$

to be compared with the quark condensate (eq. 74) which drops faster. A very important point will be discussed later. This axial-vector mixing driven by in-medium pion loop effects can be generalized for finite density [25] and is at the heart of the interpretation of the dilepton data from the NA60 collaboration (fig. 9).

**Weinberg sum rules** In complement it is possible to establish very useful sum rules, known as the Weinberg sum rules [26]. The first one is related to the spontaneous chiral symmetry breaking in the QCD vacuum and the other one is just current conservation :

$$\int_0^\infty ds \left( \rho_V(s) - \rho_A(s) \right) = f_\pi^2, \quad \int_0^\infty ds s \left( \rho_V(s) - \rho_A(s) \right) = 0. \quad (87)$$

These sum rules can be generalized at finite temperature although one needs in general the introduction of two distinct (transverse and longitudinal) spectral functions. However at fixed vanishing momentum transverse and longitudinal spectral functions coincide and the finite temperature Weinberg sum rules coincide :

$$\int_0^\infty d\omega^2 \left[ \left( -\frac{\text{Im} \Pi_V(\omega, \mathbf{q}=0)}{\pi \omega^2} \right) - \left( -\frac{\text{Im} \Pi_A(\omega, \mathbf{q}=0)}{\pi \omega^2} \right) \right] = 0 \quad (88)$$

$$\int_0^\infty d\omega^2 \omega^2 \left[ \left( -\frac{\text{Im} \Pi_V(\omega, \mathbf{q}=0)}{\pi \omega^2} \right) - \left( -\frac{\text{Im} \Pi_A(\omega, \mathbf{q}=0)}{\pi \omega^2} \right) \right] = 0 \quad (89)$$

Notice that the pion pole which appears through  $f_\pi$  in the lhs of the first sum rule at zero temperature cannot be isolated since the pion couples to other medium excitations and broadens. These sum rules will certainly give some non trivial constraints on the evolution of the shape of the spectral functions. To illustrate this point, let us play a little game and assume a simple pole Ansatz

$$-\frac{Im \Pi_V(\omega, \mathbf{q} = 0)}{\pi \omega^2} = \frac{m_\rho^4}{g_\rho^2} \frac{Z_\rho(T)}{\omega^2} \delta(\omega^2 - m_\rho^{*2}(T)) \quad (90)$$

$$-\frac{Im \Pi_A(\omega, \mathbf{q} = 0)}{\pi \omega^2} = \frac{m_A^4}{g_A^2} \frac{Z_A(T)}{\omega^2} \delta(\omega^2 - m_A^{*2}(T)) + f_\pi^{*2}(T) \delta(\omega^2) \quad (91)$$

where the masses  $m^*(T)$  are not really effective masses but have to be interpreted as the centroids of the distributions. Using these sum rules, one easily obtains the following results. First in the vacuum

$$\frac{m_\rho^4}{g_\rho^2} = \frac{m_A^4}{g_A^2}, \quad m_\rho^2 = a g_\rho^2 f_\pi^2 \quad \text{with} \quad a = \left(1 - \frac{m_\rho^2}{m_A^2}\right)^{-1} \quad (92)$$

and then at finite temperature

$$\frac{f_\pi^{*2}(T)}{f_\pi^2} = a Z_\rho(T) \left( \frac{m_\rho^2}{m_\rho^{*2}(T)} - \frac{m_\rho^2}{m_A^{*2}(T)} \right). \quad (93)$$

The conclusion is that at full restoration, where the order parameter  $f_\pi^*(T)$  vanishes, the vector and axial vector centroids are identical. But this does not tell us how the two spectral functions merge and the “big question” is how is the degeneration realized near the critical temperature  $T_c$ . Do we have a dropping scenario of quasi-particles or do we have a full melting of the resonances? This is illustrated on fig. 2. A possible mechanism is the axial-vector mixing. The emission and the absorption of thermal pions present in the hot medium is able to transform a vector current carried for instance by the  $\rho$  meson into an axial current carried by the  $a_1$  meson and at full restoration a full mixing is achieved, *i.e.*, the vector and axial correlators become identical. The same question holds at finite density where, as we will see, we also have mixing mechanisms, just replacing the thermal pions by virtual pions. Theoretical analysis of the NA60 data seem to indicate that the melting scenario is the most plausible one.

## 4 Operational approaches and effective theories for low energy QCD

### 4.1 Chiral perturbation theory

The idea and the aim of chiral perturbation theory ( $\chi PT$ ) is to construct an “exact” copy of QCD in the low energy sector for light particles whereas heavy particles are frozen or taken as static sources [27]. This is possible since there is a clear separation (mass gap)  $\Lambda_\chi = 4\pi f_\pi$  between light particles (Goldstone bosons) and heavy particles ( $\rho, \sigma, \omega, \dots$ ) which are integrated out.

To construct the effective theory (EFT) we start from two observations. The first one is that “QCD confines”. Only colorless states (hadrons) are formally introduced as fields. The second one is that chiral symmetry is spontaneously broken with the appearance of a non vanishing quark condensate which minimizes the energy of the QCD vacuum. Fluctuations around the QCD ground state are generated mainly by pions without cost of energy. We parametrize the fields associated with the fluctuations of the condensate (written in a matrix form) as :

$$M = \sigma + i \vec{\tau} \cdot \vec{\pi} \equiv S U \quad \text{with} \quad U(x) = e^{i \vec{\tau} \cdot \vec{\phi}(x)/f}. \quad (94)$$

The field  $\sigma$  and  $\vec{\pi}$ , already introduced previously in the context of the effective NJL potential, appear as the dynamical degrees of freedom and may deviate from the vacuum value,  $\langle \sigma \rangle \propto \Sigma = \langle \bar{q}q \rangle_{vac}$ , by varying external conditions (baryonic density or temperature). The potential energy (the so called chiral effective



potential) when plotted against these variables will exhibit a typical mexican hat shape (remember again the NJL model and fig. 3). The bottom is a circle (the chiral circle  $\sigma^2 + \vec{\pi}^2 = f^2$  also shown on fig. 3) in a four dimension space (analogy with the O(4) ferromagnet). The low energy constant  $f$  will be identified later with the pion decay constant  $f_\pi$ . It is convenient to go from the “cartesian” representation  $(\sigma, \vec{\pi})$  to the “polar” representation  $(S, \vec{\phi})$  as indicated in the second equality of eq. (94). The “radial” field  $S = \sqrt{\sigma^2 + \vec{\pi}^2}$  is a chiral invariant object associated with radial fluctuation of the condensate around its vacuum value  $f_\pi$ . The new pion field  $\vec{\phi}$  represents the goldstone modes associated with phase fluctuations. One moves without cost of energy on the chiral circle through these soft modes. Conversely the excitation of the radial modes cost much more energy since the associated scalar mass related to the curvature of the effective potential is a typical QCD mass (twice the constituent quark mass in the NJL model). In chiral perturbation theory the radial mode  $S$  is very naturally frozen to its vacuum expectation value,  $f_\pi$ . Only displacement on the chiral circles are thus allowed. The  $U$  matrix, parametrized in terms of the field associated with the goldstone mode, has a perfectly well defined transformation law under chiral rotations

$$U \rightarrow V_L U V_R^\dagger$$

and is the appropriate ingredient appearing in the effective lagrangian whose structure is governed by chiral symmetry alone with also the addition of the explicit symmetry breaking term.

The resulting low energy effective theory firstly describes weakly interacting pions since the interaction vanishes for zero momentum pions in the chiral limit. The QCD lagrangian is thus replaced by an effective one,  $\mathcal{L}_{eff}(U, \partial U, \partial^2 U, \dots)$ , depending on the  $U$  matrix representing the pions. This lagrangian can be organized as an expansion in powers of derivatives of the pion field or in power of pion momentum ( $p_\pi/\Lambda_\chi$ ) and in power of the quark mass or the pion mass ( $m_\pi/\Lambda_\chi$ ). To the extent that the effective lagrangian includes all terms dictated by the symmetries, the effective theory is equivalent to QCD. The leading piece is :

$$\mathcal{L}^{(2)} = \frac{f^2}{4} \text{Tr} [\partial_\mu U^\dagger \partial^\mu U] + \frac{f^2}{2} B_0 \text{Tr} [m (U + U^\dagger)]. \quad (95)$$

The first term is highly constrained by symmetry : the linear sigma model or the NJL model would give the same low energy effective theory and the  $f$  parameter has to be identified with the pion decay constant at this order. The second term is the symmetry breaking mass term. Since the quark mass is small it can be handled perturbatively, together with the power series in momentum. It is however not universal and depends on the (chiral symmetry breaking) QCD dynamics. Identifying its expectation value with the corresponding one of the true QCD lagrangian one gets  $\langle qq \rangle = -f^2 B_0$  in the chiral limit. The pion mass is identified as  $m_\pi^2 = 2m B_0$  which is nothing but the GOR relation.

To fourth order one has to construct terms allowed by symmetries :

$$\begin{aligned} \mathcal{L}^{(4)} &= \frac{l_1}{4} (\text{Tr} [\partial_\mu U^\dagger \partial^\mu U])^2 + \frac{l_2}{4} \text{Tr} [\partial U_\mu^\dagger \partial_\nu U] \text{Tr} [\partial^\mu U^\dagger \partial^\nu U] \\ &+ \frac{l_3}{4} B_0 (\text{Tr} [m (U + U^\dagger)])^2 + \frac{l_4}{4} B_0 \text{Tr} [\partial_\mu U^\dagger \partial^\mu U] \text{Tr} [m (U + U^\dagger)] + \dots \end{aligned} \quad (96)$$

The constants  $l_j$  must be determined by experiments. Given the effective lagrangian, the framework for systematic perturbative calculation of the scattering matrix involving Goldstone bosons, named Chiral Perturbation Theory (ChPT), is then defined by the following rules : *Collect All Feynman diagrams generated by  $\mathcal{L}_{eff}$ . Classify all terms according to powers of a variable  $Q$  which stands generically for three-momentum or energy of the Goldstone bosons or for the pion mass  $m_\pi$ . The small expansion parameters is  $Q/4\pi f_\pi$ . Loops are subject to regularization (most of the time dimensional) and renormalisation.* In the spirit of the EFT the unknown coefficients should be fixed by matching the EFT with QCD by renormalization group techniques but in practice they are fixed phenomenologically by comparison with data. ChPT has many successes, in first rank low energy  $\pi\pi$  scattering and the confirmation of the strong condensate scenario which validates the GOR relation. The approach can be extended quite successfully to the  $SU(3)$  sector for  $KK$  scattering. Unitarized ChPT has been also developed (for instance a ChPT amplitude is unitarized via a Bethe-Salpeter or Lippmann-Schwinger equation). This is necessary when resonances are involved since this cannot be described in perturbation theory.

Baryons can be also introduced as heavy sources coupled to pions [28]. Again the lagrangian is organized as an expansion in powers of derivatives and quark masses. The leading term is dictated by chiral symmetry alone

$$\begin{aligned} \mathcal{L}_N^{(1)} &= \bar{\psi}_N [i\gamma_\mu (\partial^\mu + iv^\mu) + g_A \gamma_\mu \gamma^5 - M_0] \psi_N \\ \text{with} \quad \xi &= \sqrt{U} \quad v^\mu = \frac{i}{2} (\xi \partial^\mu \xi^\dagger + \xi^\dagger \partial^\mu \xi) \quad a^\mu = \frac{i}{2} (\xi \partial^\mu \xi^\dagger - \xi^\dagger \partial^\mu \xi) \end{aligned} \quad (97)$$

where the Dirac spinor  $\psi_N$  denotes the iso-doublet of nucleons. There are two parameters not determined by chiral symmetry : the nucleon mass in the chiral limit  $M_0$  and the axial coupling constant  $g_A = 1.27$  known from the analysis of neutron beta decay. At next to leading order besides terms encoding the influence of the Delta in low energy pion-nucleon scattering, the symmetry breaking quark mass term appears. Its effect is to shift the nucleon mass to its physical value  $M_N = M_0 + \sigma_N$ , where  $\sigma_N \simeq 50 \text{ MeV}$  is the already encountered nucleon sigma term. An effective  $\pi N$  lagrangian can be obtained after an expansion in power of  $\vec{\phi}/f_\pi$ . It reads :

$$\begin{aligned} \mathcal{L}_{eff}^{\pi N} &= \bar{\psi}_N (i\gamma_\mu \partial^\mu - M_N) - \frac{g_A}{2f_\pi} \bar{\psi}_N \gamma_\mu \gamma^5 \vec{\tau} \psi_N \cdot \partial^\mu \vec{\phi} \\ &\quad - \frac{1}{4f_\pi^2} \bar{\psi}_N \gamma_\mu \vec{\tau} \psi_N \cdot \partial^\mu \vec{\phi} \times \partial^\mu \vec{\phi} + \frac{\sigma_N}{f_\pi^2} \bar{\psi}_N \psi_N \vec{\phi}^2 + \dots \end{aligned} \quad (98)$$

We recognize the well-known Yukawa pseudo-vector pion-nucleon coupling as the second term. The calculational framework from that, baryon chiral perturbation theory, has been applied quite successfully to a variety of low-energy processes such as threshold pion photo- and electroproduction and Compton scattering on the nucleon or pion-nucleon scattering. This approach has been extended to the chiral SU(3) dynamics. There are nice examples ( $\bar{K}N$  scattering) where the presence of resonances and in particular the  $\Lambda(1405)$  will necessitate a unitarized coupled channel approach at the price of destroying the rigorous power counting by iterating some selected subclass of diagrams. Of course ChPT has intrinsic limitations since it is a field theory which does not address the question of the nucleon structure. In other words the structure of the nucleon is hidden for what concerns for example the specific role of the pion cloud. The radial scalar field being frozen, ChPT has little to say for the nucleon mass evolution or for the real chiral origin of attractive scalar fields in nuclear matter.

## 4.2 In-medium chiral perturbation theory

**Three loop approximation.** Despite these limitations ChPT constitutes an interesting framework to address the question of the nuclear many-body problem. This approach of in-medium chiral perturbation theory involves first pions and nucleons only. The starting point is given by the pion-nucleon interaction terms given by the above ChPT lagrangian (eq. 98). However in nuclear matter a new scale appears which is the Fermi momentum  $k_F$ . Since  $k_F \approx 2m_\pi$  pions should be included as explicit degrees of freedom and the external momentum  $k_F$  has to be taken on the same footing than the pion mass.

As an example, we describe first the original work of the Munich group [29]. They calculate the EOS (the binding energy per particle) as a systematic loop expansion having a one to one correspondence with an expansion in pion mass and external momentum which is identified here with the Fermi momentum but with non trivial coefficients which are function of  $k_F/m_\pi$ . In practice this approach (which contains the effect of one-pion exchange and two-pion exchange between nucleons) is a diagrammatic approach organized according to the number of in-medium insertions at the level of the nucleon propagator :

$$S_F(p) = (\not{p} + M_N) \left( \frac{1}{p^2 - M_N^2} + 2i\pi \delta(p^2 - M_N^2) \Theta(p^0 - M_N) \Theta(k_f - |\vec{p}|) \right).$$

We refer the reader ref. [29] for details. The first contribution in the expression of the energy per nucleon is the kinetic energy and the second one is simply the Fock term of the pion exchange with two-medium insertions. The next contribution contains the iterated one pion exchange (strictly speaking the part of the diagram having two medium insertions because this diagram also has a three medium insertion including Pauli Blocking) and the last term corresponds to irreducible two-pion exchange. The corresponding

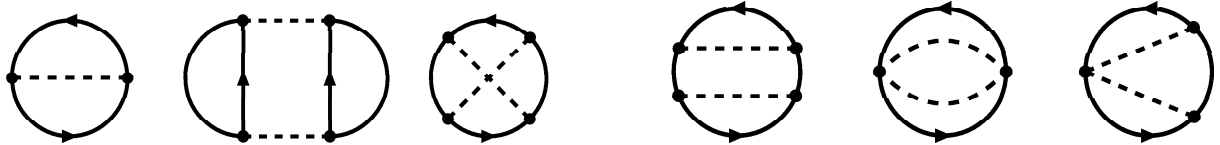


Figure 6: *One-pion exchange (1), iterated one-pion exchange Hartree (2) and Fock (3) and irreducible two-pion exchange (4,5,6) diagrams [29].*

diagrams are depicted on fig. 6. As pointed out by the authors, dimensional regularization cannot be used here since diagrams having a linear divergence would give a positive energy while standard second order perturbation theory implies attraction. For this reason they have used a cutoff which is essentially the only parameter of the calculation. The iterated exchange diagram gives the bulk of attraction through the linear cutoff dependent contribution which looks like a contact interaction. The saturation mechanism is rather unusual. It is a balance between a short range attractive interaction (going like  $\rho \propto k_F^3$ ) and intermediate range repulsion going like  $k_F^4$ . This one parameter (cutoff) calculation gives a decent saturation curve with compressibility modulus around the accepted values. Another very good point is the fact that it gives the correct asymmetry parameter. In subsequent works the effect of the  $\Delta(1232)$  resonance has been taken into account through the inclusion of one or two deltas in the intermediate state of the two-pion exchange diagrams [30]. A new scale appears which is  $\omega_\Delta = M_\Delta - M_N = 293 \text{ MeV}$  also of the order of  $2m_\pi$ , namely  $\omega_\Delta \approx k_F \approx 2m_\pi$ . This kind of diagram sometimes simulated by a fictitious sigma exchange diagram is known to give a sizable contribution to the isoscalar central part of the NN interaction. It also gives a van-der-Waal's type of interaction. Inclusion of the  $\Delta(1232)$  in more sophisticated version of the approach improves the isospin properties and in particular the energy dependence of the asymmetry energy. The real weak point of the approach at this level is that it does not reproduce the correct spin-orbit splitting which is, as everybody knows, absolutely needed to get the correct magic numbers.

**Density functional theory.** One of the traditional success of relativistic mean field theory (where the nucleon moves in the self-consistent scalar attractive and vector repulsive background fields) is to provide the appropriate spin-orbit potential since it is automatically contained in the Dirac equation for a nucleon moving in mean vector and scalar fields [31]. It is well known that the naive application of the atomic physics formula, giving a spin-orbit potential proportional to the derivative of the mean field potential, gives in the nuclear case a nuclear spin-orbit splitting too small by an order of magnitude with in addition the wrong sign. In relativistic mean field theory the saturation comes from a delicate balance between a large vector repulsion going like the ordinary density and an even larger scalar attraction depending on the scalar density which is smaller than the density. In finite nuclei the mean-field behaves roughly like the density profile and from the Dirac equation it can be shown that the spin-orbit is proportional to the algebraic difference between the vector and scalar pieces. This translates in adding the strength and this gives the appropriate enhancement and sign of the spin-orbit potential.

To incorporate this needed feature in a further work, the Munich group [32] has developed an improved approach where the nuclear ground state is characterized by strong vector and scalar mean fields and the pion loop expansion is just added on top of that. This is formulated in term of a relativistic version of the density functional theory (DFT) based on the Hohenberg-Kohn theorem which states that the energy density can be written as a functional of the density. This functional is usually decomposed first into a kinetic energy term and a Hartree exchange term associated with vector and scalar exchanges. The rest which contains the exchange Fock terms and the correlation energy is obtained from the pion loops in the chiral perturbation framework. One very attractive aspects is linked to the fact that the vector and scalar self-energies are related to QCD condensates through a (simplified) QCD sum rule analysis. One finds numerically that they just compensate for the binding energy per nucleon and they give the appropriate spin-orbit term, the bulk of the attraction coming from pion loops. However it is clear that, from the scalar self-energy, that the nucleon mass evolves just like the condensate and this cannot be true since the pion cloud piece which is about the half of the sigma commutator does not contribute to the evolution of the mass. However the whole approach gives impressively good results for finite nuclei.

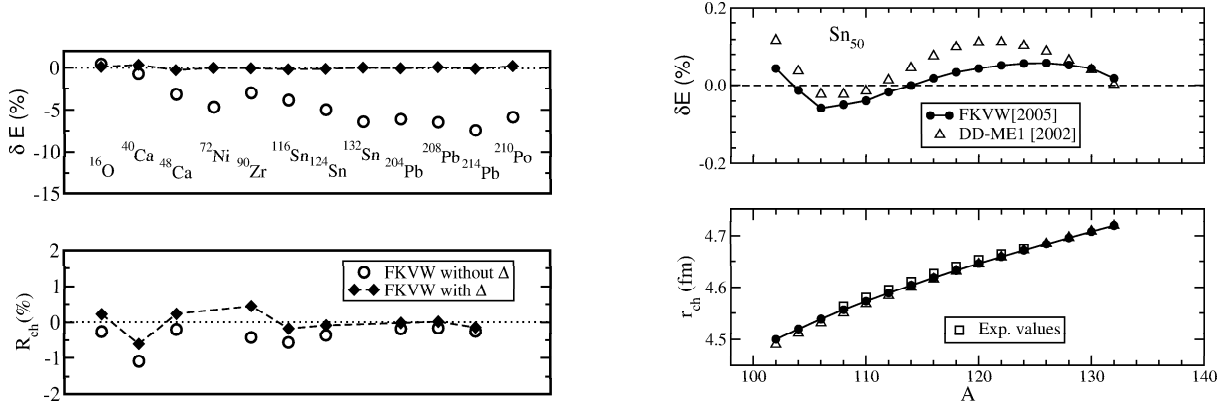


Figure 7: *Relative deviations of the calculated binding energies (upper left) and charge radii (lower left) from the experimental values for a set of spherical nuclei. Relative deviations of the calculated binding energies from the experimental values (upper right) and calculated charge radii in comparison with data (lower right) for the set of even- $A$  Sn isotopes. Details can be found in [32].*

Finite nuclei calculations are actually done using the Kohn-Sham formulation of the DFT where the ground state is built with auxiliary single particle wave functions. Minimizing the functional with respect to this wave functions give self-consistent Dirac equation for quasi-particles moving in local fields. In practice the Kohn-Sham equations are solved using an equivalent point coupling model reproducing the ChPT results. Some examples of the excellent results as good as the most sophisticated mean field relativistic approaches are shown on fig. 7. This concerns first the relative deviations of the calculated binding energy and charge radii with respect to the experimental value. It is shown that the inclusion of the  $\Delta$  significantly improves the results. The same also holds for spin-orbits splittings in doubly closed-shell nuclei. Results for an isotopic chain to test the isospin dependence in HFB calculation with a Gogny pairing force are also very good as shown on the right panel of fig. 7.

### 4.3 QCD sum rules

**Basics.** The QCD sum rule approach (QCDSR) [5] is a method which provides a relation between the fundamental properties of the QCD vacuum, namely the quark and gluon condensates, such as  $\langle \bar{q}q \rangle$ ,  $\langle (\bar{q}q)^2 \rangle$ ,  $\langle G^2 \rangle$ , and the properties of hadrons through their spectral functions (in short mass and width). It is a fully operational method in the sense that it is in principle model independent and does not require to have a real understanding on the non perturbative physics at work. The QCDSR works well for the masses of stable hadrons and also relatively sharp resonances ( $\rho$  meson,  $\Delta(1232)$ ). In hadron spectroscopy, QCDSR plays a complementary role to the lattice QCD since both extract hadron masses from two-point correlation functions. The basic object is a two-point correlator between two currents (or interpolating fields) having the quantum numbers of the hadron under consideration. As already seen, using essentially causality, the correlator in momentum space is expressed as a dispersive integral involving the spectral function which is the object experimentally observable via appropriate probes like  $\gamma$ ,  $W^\pm$  :

$$\Pi(q^2) = \frac{i}{3} \int d^4x e^{iq \cdot x} \langle 0 | \mathcal{T} (J^\mu(x), J_\mu(0)) | 0 \rangle = \Pi(0) + q^2 \int_0^\infty \frac{ds}{s} \frac{\left(-\frac{1}{\pi}\right) \text{Im} \Pi(s)}{q^2 - s + i\eta} \quad (99)$$

We have taken here the specific case of the electromagnetic current which can be decomposed according to its quark content into  $\rho$ ,  $\omega$  and  $\phi$  components :

$$J^\mu = \frac{2}{3} \bar{u} \gamma^\mu u - \frac{1}{3} \bar{d} \gamma^\mu d - \frac{1}{3} \bar{s} \gamma^\mu s = J_\rho^\mu + J_\omega^\mu + J_\phi^\mu \quad (100)$$

$$J_\rho^\mu = \frac{1}{2} (\bar{u} \gamma^\mu u - \bar{d} \gamma^\mu d), \quad J_\omega^\mu = \frac{1}{6} (\bar{u} \gamma^\mu u + \bar{d} \gamma^\mu d), \quad J_\phi^\mu = -\frac{1}{3} \bar{s} \gamma^\mu s. \quad (101)$$

The three associate spectral functions  $(\rho, \omega, \Phi)$  can be measured by looking at various hadronic channels in  $e^+e^-$  annihilation since it is experimentally established that these different channels which interfere weakly are strongly dominated at low energy by the corresponding resonances :

- $J_\rho^\mu$  :  $\rho$  dominance through  $e^-e^+ \rightarrow \rho \rightarrow \pi\pi$
- $J_\omega^\mu$  :  $\omega$  dominance through  $e^-e^+ \rightarrow \omega \rightarrow 3\pi$
- $J_\Phi^\mu$  :  $\Phi$  dominance through  $e^-e^+ \rightarrow \Phi \rightarrow K\bar{K}$ .

It follows that this correlator is known for any value of  $q^2$  once we know the spectral function  $\rho(s) = -(1/\pi s) \text{Im}\Pi(s)$ .

For large space like momenta  $Q^2 = -q^2 = \bar{q}^2 - q_0^2 \rightarrow +\infty$ , the correlator is dominated by small size configurations for which perturbative QCD is applicable. In practice this is done using the so-called Operator Product Expansion (OPE) [33] which is a Taylor expansion around  $x = 0$  of the space-time correlator. In momentum space one obtains a dominant log term plus an expansion in  $1/Q^2$  with coefficients involving quark and gluon condensates, *i.e.*, matrix elements of quark and gluon operators on the non perturbative QCD vacuum :

$$\begin{aligned} \frac{\Pi(q^2 = -Q^2)}{Q^2} &= \int_0^\infty \frac{ds}{s} \left( -\frac{1}{\pi} \right) \frac{\text{Im}\Pi(s)}{s + Q^2} \\ &= \frac{d_V}{12\pi^2} \left[ -c_0 \ln\left(\frac{Q^2}{\mu^2}\right) + \frac{c_1}{Q^2} + \frac{c_2}{Q^4} + \frac{c_3}{Q^6} + \dots \right]. \end{aligned} \quad (102)$$

The momentum  $\mu$  is an arbitrary scale usually chosen around  $1 \text{ GeV}$ . In the isovector channel ( $\rho$  meson channel,  $d_V = d_\rho = 3/2$ ) one finds

$$\begin{aligned} c_0^\rho &= 1 + \frac{\alpha_S(Q^2)}{\pi}, \quad c_1^\rho = -3(m_u^2 + m_d^2), \\ c_2^\rho &= \frac{\pi^2}{3} < G \cdot G > + 4\pi^2(m_u < \bar{u}u > + m_d < \bar{d}d >) \\ c_3^\rho &\sim \text{“Four-quark condensates”} \sim < (\bar{q}q)^2 > \end{aligned} \quad (103)$$

where  $\alpha_S(Q^2) \simeq 4\pi/[9 \ln(Q^2/\Lambda_{QCD}^2)]$  is the QCD running coupling. At this point we do not give the explicit form of  $c_3$  in terms of the four-quark condensates but simply mention that their values are not so well known. Consequently a factorization,  $< (\bar{q}q)^2 > \sim < \bar{q}q >^2$ , is often assumed which constitutes one of the major uncertainties of the method. In the next subsection we will nevertheless say a little bit more about this specific point. For the  $\omega$  meson ( $d_\omega = 1/6$ ) the only modification concerns the  $c_3$  parameter. The equation (102) contains the desired link between QCD condensates (rhs) and hadron properties (lhs) but there is an important difficulty. The OPE converges only for large  $Q^2$  but in that case many resonances contribute to the dispersive integral and the information on the low lying resonances is partially lost. To improve the weight of the low mass resonances and the convergence of the OPE one uses a trick which is a change of variables ( $Q \rightarrow M_B$ ) called Borel transform. A new equation is obtained :

$$\frac{1}{M_B^2} \int \frac{ds}{s} e^{-s/M_B^2} \left( -\frac{1}{\pi} \right) \text{Im}\Pi(s) = \frac{d_V}{12\pi^2} \left[ c_0 + \frac{c_1}{M_B^2} + \frac{c_2}{M_B^4} + \frac{c_3}{2M_B^6} + \dots \right]. \quad (104)$$

The improvement lies in the fact that the high part of the spectrum is now exponentially suppressed. The consistency test of the method is a relatively large optimum domain in the Borel mass in which the lhs and the rhs of eq. (104) coincide, with  $M_B$  not too large to reinforce the low part of the spectrum and not too small to have the convergence of the OPE. The test of coherence of the method is a sufficiently large domain in the Borel mass, typically  $0.8 \text{ GeV} - 1.5 \text{ GeV}$ , in which the rhs and lhs coincide.

In the vacuum the lhs involving the spectral function can be taken either from data or from a model. The QCDSR analysis allows to extract the value of the condensates. An example has been given above which concerns the energy density of the QCD vacuum related to the value of the gluon condensate extracted from charmonium sum rules. It turns out that in general the analysis is not very sensitive to the width

of the resonances provided it is not too large. The conventional sum rule analysis assumes a specific form for the spectral function, usually a pole plus continuum assumption :

$$R(s) = -\frac{12\pi}{s} \text{Im} \Pi(s) = \mathcal{F}_V \delta(s - m_V^2) + d_V \left(1 + \frac{\alpha_S}{\pi}\right) \Theta(s - s_V) \quad (105)$$

The simplified spectral function is made of a peak at the vector meson mass and a perturbative QCD continuum beyond a characteristic scale  $s_V$  with  $d_\rho = 3/2$ ,  $d_\omega = 1/6$ ,  $d_\Phi = 1/3$ . The inverse work can be done. From the known condensates, optimal values of  $(s_V, m_V, \mathcal{F}_V)$  can be determined. One finds  $s_{\rho,\omega} = 1.5 \text{ GeV}^2$ ,  $s_\Phi = 2.2 \text{ GeV}^2$ , which yields almost exactly the experimental values  $m_{\rho,\omega} = 0.77 \text{ GeV}$ ,  $m_\Phi = 1.02 \text{ GeV}$ . The fact that the approximate degeneracy of the  $\rho$  and  $\omega$  meson masses emerges naturally in the OPE is one of the traditional successes of the QCDSR.

**In-medium QCD sum rules.** The QCDSR approach can be generalized at finite density but Lorentz invariance is lost and there is a separate dependence of spectral functions on the energy  $q^0 = \omega$  and the three momentum  $\vec{q}$ . At  $\vec{q} = 0$  the QCDSR equation has nevertheless the same form than in vacuum and a similar analysis can be made but including the density dependence of the condensates. Again the main uncertainty is the four-quark condensate for which a not very well controlled factorization approximation is made. At this level we stress that the naive application of QCDSR at finite density may be dangerous when strong melting of the meson resonances with other many-body excitations occur. This is the case for the rho meson where an erroneous dropping mass scenario was proposed in the past on the basis of a too simplistic QCDSR analysis. We will come to this point in the next subsection.

#### 4.4 In-medium hadrons

**Status of the problem.** Intense theoretical and experimental activities have been devoted in the recent years to the question of the in-medium changes of hadrons or more precisely to the evolution with density and temperature of correlators and spectral functions. It is rather suggestive that the properties of a composite object such as a hadron are modified once it is placed in a piece of matter (e.g., a nucleus) or in a heat bath (e.g., a fireball emerging in a relativistic heavy-ion collision). At least if the density of the system is so high that the size of the composite object is comparable to the average distance between the constituents of the system, then the intrinsic structure of the composite object starts to play a role. The strongly interacting medium can be seen as a QCD system which is characterized by modified properties, *i.e.* modified condensates. This may be linked to a modified symmetry pattern of QCD associated with (partial) chiral restoration. This change of the “QCD ground state” is expected to be “visible” in the modification of its excitation spectrum, namely the hadrons through their mass, width or coupling constants. However the in-medium changes of hadrons (the associated correlation functions) are usually calculated within conventional hadronic many-body approaches based on chiral dynamics where hadrons move in the implicitly unmodified chirally broken vacuum. In short, the central question is thus to make a connection between the observed or calculated in-medium changes of hadrons and (precursor) effects of chiral restoration. A priori the QCDSR approach seems to be ideally suited for this job. Indeed the QCD sum rule, when generalized at finite density, allows to relate the evolution of the hadron spectral functions to the changes of the QCD condensates. However the less satisfactory point is that this approach only constrains but does not elucidate the precise nature of physical mechanisms driving chiral restoration. The QCDSR should be mixed with more detailed approaches (models, effective theories, lattice). In the next paragraph we will give a brief and non exhaustive review of some prominent medium effects and in particular those related to the  $\rho$  meson.

**Some examples of medium effects.** In the nuclear medium the pion propagation is modified mainly from its p-wave interaction with nucleons (the second term of the first line of the effective lagrangian given in eq. 98). For sufficiently energetic pions ( $\omega \approx 300 \text{ MeV} \approx M_\Delta - M_N$ ) the  $\Delta(1232)$  can be also excited and it is the dominant process. These virtual particle-hole and delta-hole excitations are represented on fig. 8. The problem of pion propagation in nuclear matter possesses a strong analogy with the propagation of light in matter, the delta excitation playing the role of the dipole excitation of atoms which modifies the dispersion relation of in-medium photon [34]. Most of the physics can be captured

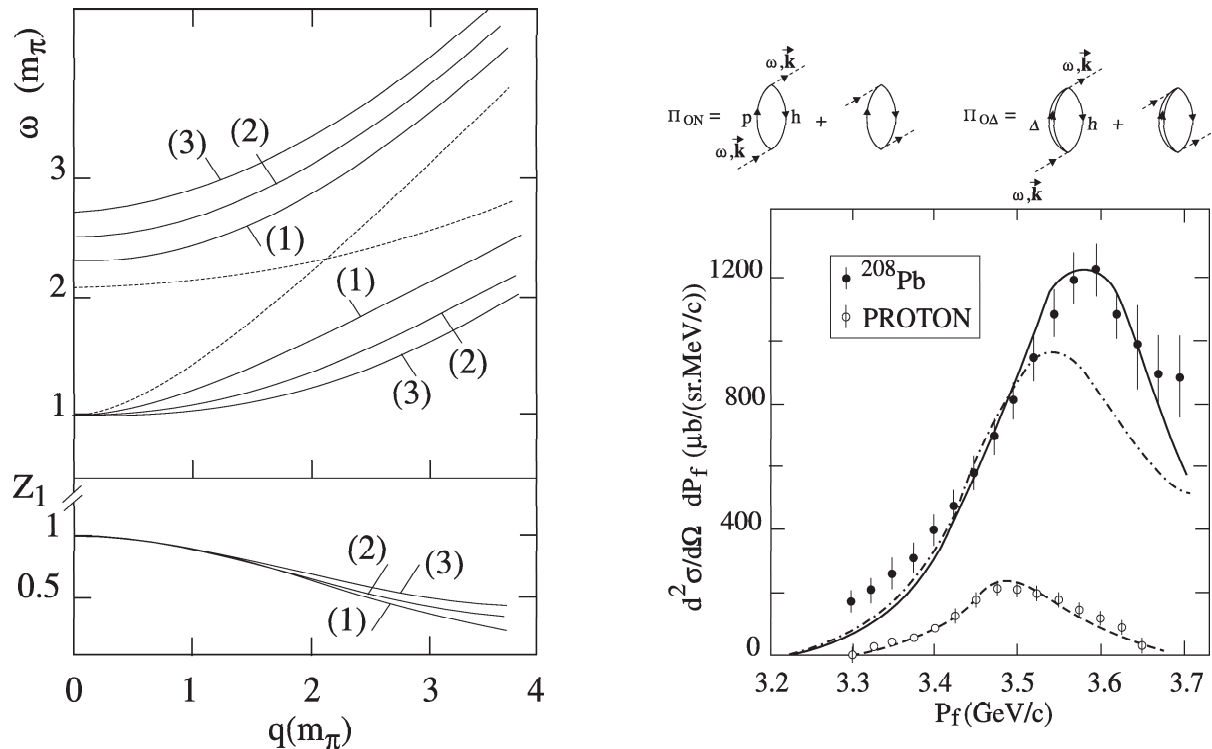


Figure 8: *Light panel: on the upper part the dispersion curves for the pionic collective modes are shown for various values of  $\rho/\rho_0$ ; the pionic branch corresponds to the lowest mode; on the lower part the strength of the pionic branch (not discussed in the text) is shown. Upper right panel: virtual  $p-h$  and  $\Delta-h$  excitations modifying pion propagation. Lower right panel: comparison of theory to experiment for  $\Delta$  excitation in  $^{208}\text{Pb}$  by the  $(^3\text{He}, t)$  reaction at 2 GeV and zero angle; the dot-dashed curve is the first order response and the full curve includes collective  $\pi\Delta$  effects; the dashed curve corresponds to a calculation on a proton target [36].*

by a simple two-level quantum mechanical model [35] which also incorporates the effect of short-range correlations (the Ericson-Ericson-Lorentz-Lorenz (EELL) effect). There are two physical collective modes whose dispersion relations are depicted on fig. 8 at various densities. In particular the lowest one called the pionic branch is significantly softened with respect to the free pion one. Within a much more detailed approach adapted for finite nuclei [36] a convincing interpretation of the observed shift of the strength in the  $(^3\text{He}, T)$  experiment at SATURNE has been given in term of this pionic branch as shown on the right panel of fig. 8.

Since the pions are softened in nuclear matter it has been proposed that the two-pion states or two-pion resonances should be also softened in nuclear matter [35, 37]. This concerns in first rank the sigma meson. We mean here by sigma meson the  $f_0(600)$  of the particle booklet which is plausibly a broad  $\pi\pi$  resonance which has probably little relation with the chiral partner of the pion discussed above. Such an object can be generated by unitarized chiral perturbation, *i.e.*, chiral dynamics. Various collaborations have measured the invariant mass distribution for a produced pion pair in a reaction induced either by incoming pions or photons on various nuclei. They have all observed a systematic  $A$  dependent downwards shift of the strength when the pion pair is produced in the scalar-isoscalar channel namely in the sigma meson channel. As a specific example, photo-production data of the TAPS collaboration at MAMI [38] clearly exhibits a downwards shift of the strength growing up from hydrogen to lead in the  $\pi_0\pi_0$  channel dominated by the sigma meson channel and this effect is not present in the isospin one channel. The explanation relies on the medium modification of the two-pion propagator and consequently the unitarized  $\pi\pi$  interaction induced by the softening of the single pion dispersion relation. A full calculation along

these lines has been performed by the Valencia group in a framework of unitarized chiral perturbation theory [39] which not badly reproduces the data. The “big question” of the connection with chiral symmetry restoration has been intensively debated. Quite superficially there is a very general argument since chiral restoration implies a softening of a collective scalar-isoscalar modes in agreement with the data. Moreover it turns out that the medium effects governing the reshaping of the strength in the low invariant mass region in two-pion production experiments are precisely the same as those affecting the scalar susceptibility and accelerating its convergence with the chiral partner pseudo-scalar susceptibility as shown on fig. 5 [22].

**The in-medium rho meson spectrum and chiral restoration.** We have already seen in section 4.3 that the iso-vector vector correlator, *i.e.*, the iso-vector piece of the correlator of the electromagnetic current is saturated at low energy by the  $\rho$  meson. This so-called vector dominance (VDM) is formally described in its simplest form by a field current identity which states that the hadronic electromagnetic current is proportional to the vector meson field :  $J_\rho^\mu = (m_\rho^2/g_\rho) \rho^\mu$  with  $g_\rho \simeq 5$ . The physical meaning is that the coupling of a photon to hadrons is not direct but proceeds through the transformation of a (virtual) photon into a rho meson which couples to hadrons. This well established phenomenological observation opens the possibility of studying the rho meson spectral function in excited strongly interacting matter (formed for instance in relativistic heavy ion collisions) by measuring electromagnetic radiations, *i.e.*, dileptons arising from virtual (time-like) photons,  $\gamma^* \rightarrow \mu^+\mu^-$  or  $e^+e^-$ .

The VDM phenomenology can be easily implemented in effective chiral Lagrangians. An example used in ref. [40] is a gauged non linear sigma model lagrangian :

$$\mathcal{L}_{\rho h} = -g \vec{\rho}^\mu (\vec{\Phi} \times \partial_\mu \vec{\Phi}) - g \bar{N} \gamma_\mu \vec{\rho}^\mu \cdot \frac{\vec{\tau}}{2} N - g \frac{g_{\pi NN}}{M_N} \bar{N} \gamma_\mu \gamma_5 (\vec{\rho}^\mu \times \vec{\Phi}) \cdot \frac{\vec{\tau}}{2} N + \frac{g^2}{2} (\vec{\rho}^\mu \times \vec{\Phi}) \cdot (\vec{\rho}_\mu \times \vec{\Phi}) \quad (106)$$

The vacuum width of the rho meson,  $\Gamma = 150 \text{ MeV}$ , comes from its decay in two pions controlled by the coupling constant  $g$ . In the medium the  $\rho$  will decay into in-medium modified collective quasi-pions. As in the case of the scalar modes, due to the softening of the pion dispersion relation, this generates an accumulation of strength for an invariant mass near  $2m_\pi$ . This is the first diagram depicted on the upper left panel of fig. 9. The other two diagrams are permitted by the presence of the third term of the lagrangian (106), the Kroll-Ruderman (KR) term required by gauge invariance. The first KR diagram is a vertex correction with a polarization  $\Delta$ -hole bubble which just kills the structure at  $2m_\pi$  and the last one generates a structure near  $500 \text{ MeV}$  through the decay of the rho into a quasi-pion (the pionic branch or the lowest mode of fig. 8) and a  $\Delta$ -hole state. This constitutes our original prediction of ref. [40] shown on the lower left panel of fig. 8 where we clearly see a structure growing up below the rho peak with increasing density. This model has been subsequently improved in collaboration with R. Rapp and J. Wambach [41, 42] and developped [43, 44] by the adjunction of the direct coupling of the rho meson to higher baryonic resonances (in particular the  $N^*(1520)$ ) on top of the pion cloud effect and adapted to the context of relativistic heavy ion collisions and dilepton production. After more than ten years of intensive theoretical and experimental activities, the NA60 collaboration [45] has been able to really extract the rho meson spectral function as shown on the lower middle panel of fig. 9. The unmodified rho as well as the dropping rho scenario are clearly ruled out. The data show a sizable broadening in agreement with the theoretical framework discussed above, now referred as the Rapp-Wambach (RW) scenario. The original pion cloud effect is one contributor explaining part of the strength below the rho peak. This broadening is sometimes put forward as a signature of chiral symmetry restoration but again the “big question” arises. Is it possible to identify mechanisms directly connected with chiral restoration? The answer is yes since we have demonstrated in ref. [25] that the pion cloud contribution, which is mainly driven by the baryonic density, contains an axial-vector mixing effect (see also the discussion at the very end of section 3). The rho meson mixes with the finite density axial correlator which has a pionic contribution and a baryonic contribution carried by  $\Delta$ -hole states. Finally there are pure meson gas contributions, referred as  $4\pi$  mixing [46] on the lower right panel of fig. 9 which populate the tail beyond the rho peak. They also contain an explicit mixing between the  $\rho$  meson and the  $a_1$  meson.

As discussed in the introduction of the sub-section, QCDSR may provide a connection between hadron spectral functions and fundamental changes in the QCD vacuum. In a recent work [47], an interesting



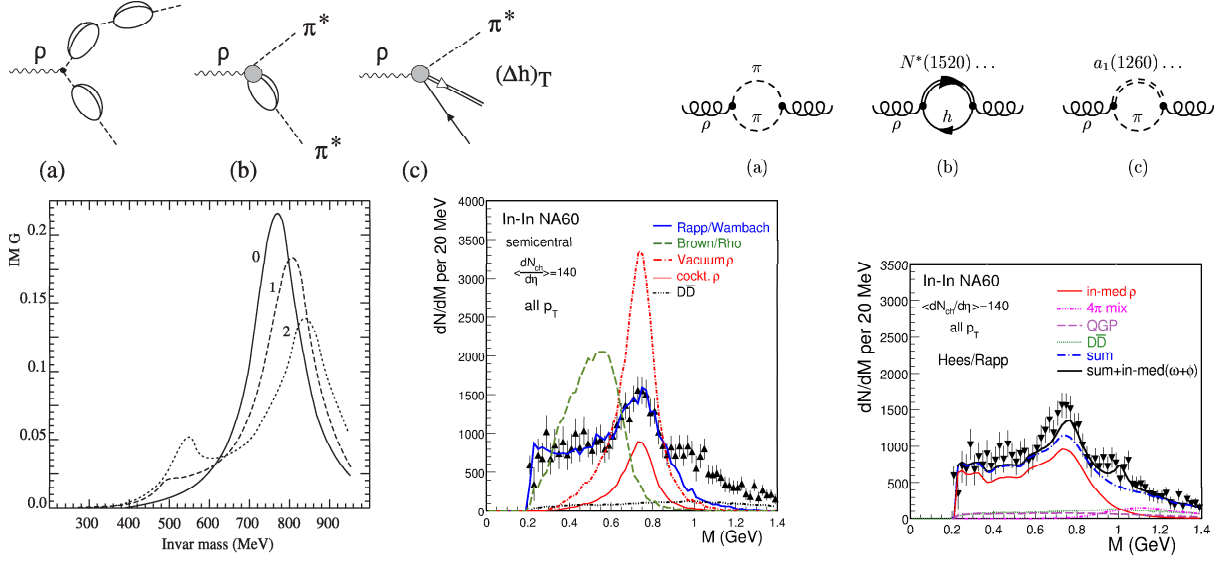


Figure 9: *Upper panel: medium corrections to the rho propagation as explained in the text (left); the right part summarizes the self-energy diagrams of the rho meson: pion cloud effect (a) , direct coupling to baryonic (b) and mesonic (c) resonances. Lower panel: original prediction [40] for the rho meson spectral function at various values of  $\rho/\rho_0$  (left); NA60 dimuon spectrum [45] in semi-central In(158 AGeV)-In collisions compared to theoretical predictions from the Rapp-Wambach scenario (middle); the theoretical calculation presented on the right part also incorporates the effect of chiral mixing [46].*

QCDSR analysis for the  $\rho$  meson spectral function has been performed. The aim was to study the compatibility of either a pure dropping rho mass or a pure broadening scenario with the evolution of the QCD condensates in a pure chiral restoration scenario. Pure chiral restoration means that only the chirally odd condensates which are not chiral invariant drop to zero at full restoration since they have to be zero by definition of a chiral order parameter. The other symmetric condensates may also drop but this is not required by chiral symmetry alone. The pure chiral restoration assumes that these symmetric condensates which are chirally even remain at their vacuum value. According to the discussion given in subsection 4.3, the important condensates are the gluon condensate and the four quark condensate. The gluon condensate entering the  $c_2$  coefficient in eq. (102, 103) is chirally symmetric : it keeps its vacuum value. The four-quark condensate entering the  $c_3$  coefficient can be split in a symmetric piece remaining at its vacuum value and a chirally odd piece. It has been shown that the ALEPH data in vacuum [23] are compatible with the factorization of this chirally odd chiral condensate according to  $\langle \mathcal{O}_4^{br} \rangle \approx (9/7) \langle \bar{q}q \rangle_{vac}^2$ . For the pure chiral restoration scenario one drops it to zero at full restoration. Written schematically, the ansatz for the  $\rho$  meson spectral function is taken as  $-ImD_\rho(s) \propto [(s - m_0^2)^2 + \Gamma_0^2 F(s)]^{-1}$ , where  $F(s)$  is a purely kinematical function. In the vacuum the QCDSR is compatible with  $(m_0, \Gamma_0) = (775 MeV, 149 MeV)$ . The QCDSR at full restoration is compatible with an increased width parameter  $\Gamma_0$  provided the rho meson mass parameter  $m_0$  is dropped accordingly. This generates a curve,  $m_0(\Gamma_0)$ , depicted on the left panel of fig. 10, compatible with the pure chiral restoration. Two extreme cases are possible. (i) The width remains at its vacuum value, the mass drops and the spectral function shown on the right panel is significantly shifted downwards around 600 MeV. (ii) The opposite interpretation is conceivable as well, namely pure but considerable broadening with keeping the vacuum value of the rho meson peak. The data seem indeed to favor such a broadening effect. Conversely one can say that the data are not incompatible, at least at a qualitative level, with a pure chiral restoration scenario.

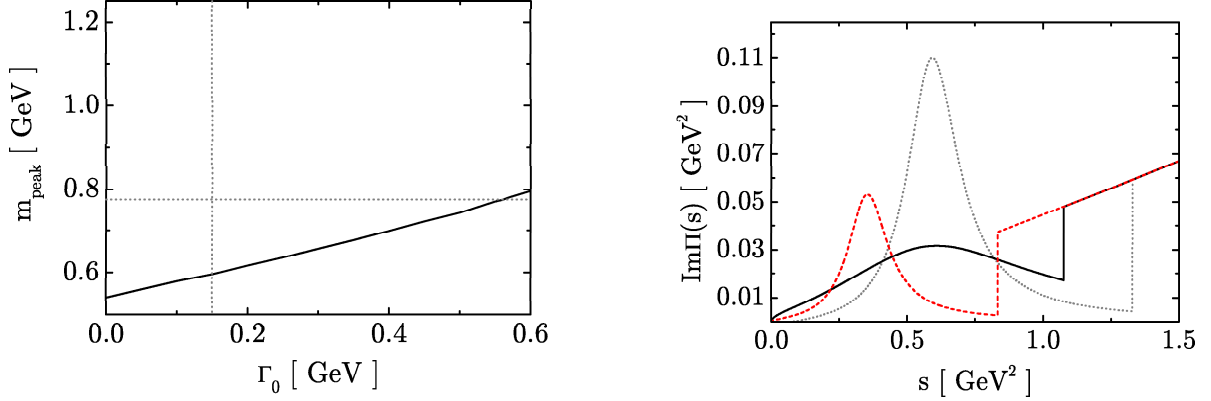


Figure 10: *Left panel: peak position of the rho meson spectral function as a function of the width parameter; the dotted lines mark the experimental vacuum values. Right panel: the rho meson spectral function in the vacuum case (dotted curve) and in the pure chiral restoration scenario for the width fixed at its vacuum value (dashed curve) or the mass fixed at its vacuum value (solid curve). All these results are taken from [47].*

## 5 Thermodynamics of QCD

### 5.1 QCD phase diagram and chiral symmetry

To describe the thermodynamics and the phase structure of QCD, we prefer to use a representation where the variables are intensive variables, namely the temperature  $T$  and various chemical potentials  $\mu$  associated with conserved quantities, essentially here the baryon number. The pressure  $P$  which is also an intensive quantity is actually a function of  $T$  and  $\mu$  (sometimes referred as  $\mu_B$ ) and this constitutes the equation of state (EOS). One reason for this choice is that for any system in thermodynamic (thermal, mechanical and chemical) equilibrium,  $T$ ,  $P$  and  $\mu$  have to be uniform within the various subsystems in particular in case of phase coexistence. Another reason is that lattice calculations are performed using  $T$  and  $\mu$  as independent control parameters (in a grand canonical ensemble). Finally heavy ions data are often analyzed in terms of these variables. This concerns for instance particle production from a thermal source and fireball evolution constrained by conservation laws.

From the thermodynamical relations in a uniform system one has  $dP = \sigma dT + \rho d\mu$  from which the density of extensive quantities, (entropy density  $\sigma$ , baryon number density  $\rho$ , energy density  $\epsilon$ ) can be obtained :

$$\sigma = \frac{S}{V} = \left( \frac{\partial P}{\partial T} \right)_{\mu}, \quad \rho = \frac{N}{V} = \left( \frac{\partial P}{\partial \mu} \right)_T, \quad \epsilon = \frac{E}{V} = T\sigma + \mu\rho - P. \quad (107)$$

By contrast those quantities can differ from one phase to another phase. In particular in case of a first order transition for a given  $(T, \mu)$  two different phases with two different values of mechanical quantities  $(\rho_1, \epsilon_1)$  and  $(\rho_2, \epsilon_2)$  can exist simultaneously. It is convenient to represent the phase diagram in the  $(T, \mu)$  plane, as shown on the lower panel of fig. 11. The phase coexistence line starting at zero temperature terminates at a certain critical point  $(T_C, \mu_C)$  where there is no longer discontinuity in  $\rho, \epsilon$ . At this point the susceptibilities (second derivatives of the pressure, namely heat capacity and the baryon number susceptibility),

$$C = T \left( \frac{\partial \sigma}{\partial T} \right)_{\mu}, \quad \chi_B = \left( \frac{\partial \rho}{\partial \mu} \right)_T, \quad (108)$$

may diverge, e.g.,  $C \sim |T - T_C|^{-\alpha}$ . The positive number  $\alpha$  is the critical exponent associated with the heat capacity. This is characteristic of a second order transition. The well known example is the liquid-gas transition of water or nuclear matter.

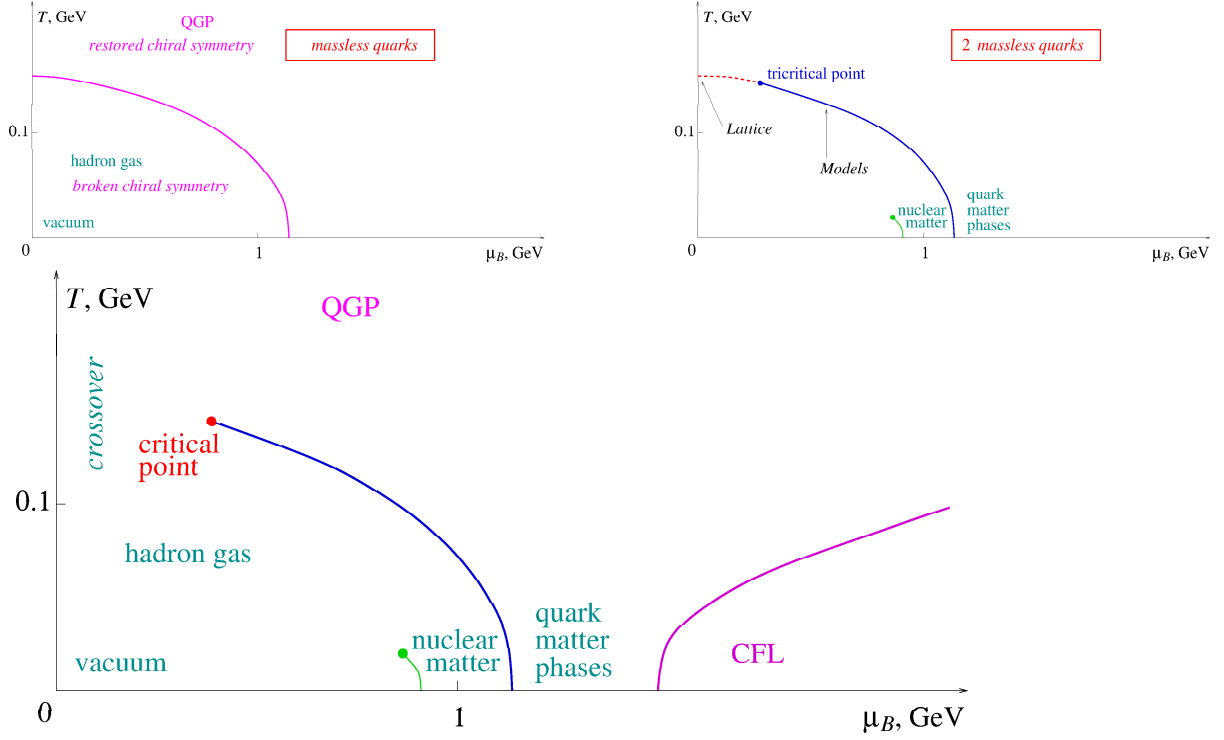


Figure 11: Upper panel: phase diagram of QCD with three massless quarks (left) and two massless and one massive quarks (right). Lower panel: the contemporary view of the QCD phase diagram with physical quark masses - a semiquantitative sketch. Taken from [48].

In QCD and in other systems like spin systems, there is another aspect which is linked to symmetries. In the QCD case this concerns the already discussed chiral symmetry in the limit of vanishing quark masses. It may exist phases which differ by the way the symmetry is realized.

- The symmetry is spontaneously broken: the state of the system cannot be characterized only by  $(\rho, \epsilon)$  since a chiral transformation will map the ensemble  $(\rho, \epsilon)$  on itself. It is necessary to specify the state by a quantity which is not invariant under the symmetry transformation, namely an order parameter. An example is the chiral or quark condensate.

- The symmetry is trivially realized or restored. The order parameter must vanish.

In the particular case of QCD, due to the specific form of the chiral symmetry breaking piece, the order parameter can be obtained from the derivative of the pressure with respect to the symmetry breaking parameter :

$$\langle H_{\chi SB} \rangle = \int d^3r 2m \langle \bar{q}q \rangle \Rightarrow \langle \bar{q}q \rangle = -\frac{1}{2} \left( \frac{\partial P(T, \mu, m)}{\partial m} \right)_{T, \mu}. \quad (109)$$

The transition can be very well a first order one with different  $(\rho, \epsilon)$  and the the order parameter is discontinuous. However it may happen that all the first derivatives of the pressure, which is now a function of  $T, \mu$  and  $m$ , remains continuous but, since the transition connects two states with different symmetry patterns, the partition function and thermodynamic quantities exhibit a non analytical behaviour. In this case the susceptibilities (second derivatives of the pressure) can be discontinuous or even diverge. The susceptibility of the order parameter, is the scalar or chiral susceptibility :  $\chi_S = (\partial \langle \bar{q}q \rangle / \partial m)_{T, \mu}$ .

On the transition line it behaves as  $\chi_S = |T - T_c|^{-\nu(2+\eta)}$  whereas the correlation length diverges as  $\xi = |T - T_c|^{-\nu}$ ,  $\nu$  and  $\eta$  being other critical exponents. One of the remarkable consequences of the renormalization group is the universality class of the critical phenomena. Indeed the critical exponents such as  $\alpha, \nu, \eta$  do not depend on the detailed microscopic nature of the underlying theory. They fall into universality classes which depend only on general properties such as dimensionality or symmetry. For

those values of  $\mu$  for which the chiral restoration in two-flavor ( $N_f = 2$ ) massless QCD is of second order, the universality class is the one of the  $SU(2) \otimes SU(2) \sim O(4)$  linear sigma model for which  $\nu = 0.75$  and  $\eta = 0.04$ . The order parameter behaves as  $|T - T_c|^\beta$  with  $\beta = \nu(1 + \eta)/2 = 0.39$ .

In the limit of three massless or very light ( $u, d, s$ ) quarks, universality arguments and lattice results seem to demonstrate that criticality cannot exist and the  $SU(3)_L \otimes SU(3)_R$  chiral restoration transition must be always of first order. One obtains a first order transition line shown on the upper left panel of fig. 11. In the limit of vanishing  $u$  and  $d$  quark masses and a heavier strange quark mass the symmetry reduces to  $SU(2)_L \otimes SU(2)_R$  and a first order transition is expected to occur at large  $\mu$  and low  $T$ , as shown on the upper right panel of fig. 11. The first order line (full line) terminates at a point called the tricritical point (TCP) located at a certain  $(T_{TCP}, \mu_{TCP})$ . Beyond this point ( $\mu < \mu_{TCP}$ ,  $T > T_{TCP}$ ), since one has non analytical behaviour of thermodynamic quantities, a second order phase transition (dashed line) described just above is expected. The location of this TCP is a very important theoretical question motivating lattice studies.

For physical quark masses (lower panel of fig. 11) the chiral symmetry is explicitly broken. There is still a first order transition line (full line) which terminates at a critical end point (CEP) located at a certain  $(T_{CEP}, \mu_{CEP})$ . This type of critical point is the most common one and corresponds to the Ising model or liquid-gas phase transition universality class. Beyond the CEP ( $\mu < \mu_{CEP}$ ) the transition from low temperature to high temperature phases cannot proceed through a singularity. Lattice simulations indeed show that this transition is a continuous (although sudden) crossover a little bit like in water where the singularity occurs only near the CEP. What distinguishes the hadron gas (liquid water) from the quark gluon plasma (vapor) is only quantitative, one is denser than the other. The similarity with water also occurs in the low temperature sector when a number of ordered (crystalline) quark phases must exist which are akin to many confirmed forms of ice. In a three dimensional diagram  $(\mu, T, m)$  one has a surface of first order transition which terminates on a line of second order CEP which emanates from the tricritical point (CEP) where  $\langle \bar{q}q \rangle \approx |T_{CEP} - T|^{1/4}$  in the mean-field Landau-Ginzburg theory. QCD thermodynamics can be studied by lattice QCD calculations. Since this is a very rapidly evolving domain we will give some results or numbers only for indication. We thus urge the reader, when reading the lectures, to look at the most recent publications to have up-to-date results. These numerical simulations reveal that, for physical quark masses, chiral symmetry is restored at vanishing chemical potential by a smooth crossover transition. The RBC-Bielefeld-HotQCD group [12] finds a chiral transformation around temperature  $T \sim 185 - 195 \text{ MeV}$ . The important point is that it is accompanied by the deconfinement transition as corroborated by many observables. However The Wuppertal-Budapest group [49] finds a larger deconfinement temperature compared to the chiral one by examining the peaks of the chiral loop and the Polyakov loop susceptibilities. This question of the deconfinement transition and the associated notion of Polyakov loop will be discussed in a next subsection. The location of the critical end point is also the subject of lattice investigations. It is nevertheless still an open question since lattice calculations at small quark masses and finite chemical potential suffer from important technical difficulties. We quote here as representative numbers the result of ref. [50] :  $(T, \mu)_{CEP} = (162 \pm 2 \text{ MeV}, 360 \pm 40 \text{ MeV})$

## 5.2 Connection with relativistic heavy ion collisions

In a relativistic heavy ion collision the colored quarks and gluons are produced by primary nucleon-nucleon collisions. These colored objects will immediately re-interact to form hadrons in case of isolated  $NN$  collisions. However in the case of high energy nuclear collisions, before being fully formed hadrons, the pre-hadronized clusters run into a secondary generation of subsequent collisions within the nuclear density distribution of the heavy nuclei. The process may continue up to an thermally equilibrated phase of matter made of colored quarks and gluons : the Quark-Gluon-Plasma (QGP). Indeed results at RHIC top-energies ( $\sqrt{s_{NN}} = 200 \text{ GeV}$ ) suggest that such a new form of partonic matter is created and it is locally equilibrated early-on because of its hydrodynamic expansion pattern. Three major discoveries can be cited: the large azimuthal anisotropy of particle emission in non central collisions (elliptic flow) favoring a strongly interacting perfect fluid (sQGP), the scaling of this anisotropy with the number of constituent quarks (constituent quark scaling) and the suppression of high energetic particles traversing the medium (jet quenching). The minimal conclusion which can be drawn is that the phase boundary is traversed in a relativistic nucleus-nucleus collision. Moreover the perfect fluid formation and the jet

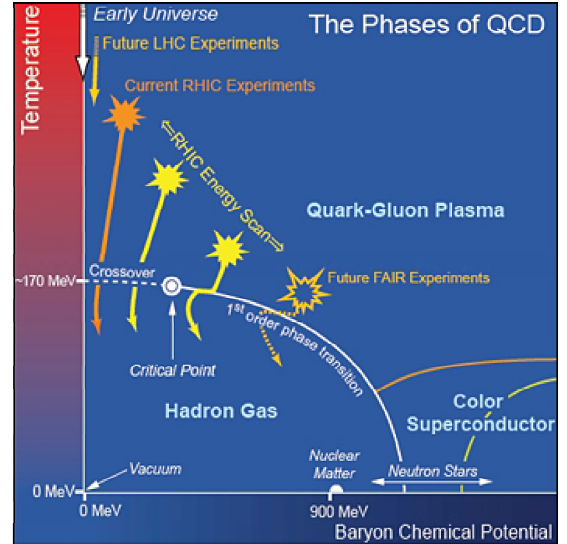
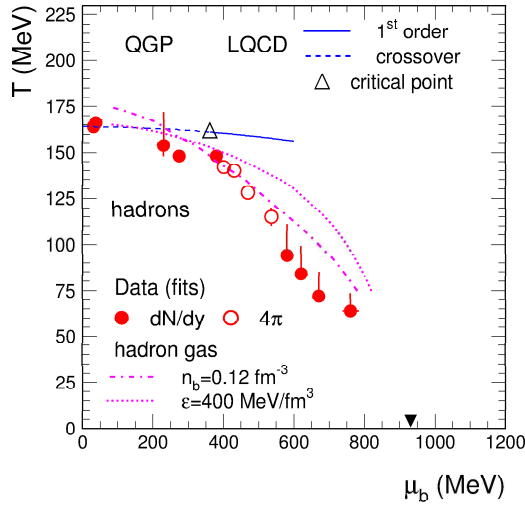


Figure 12: *Right panel: the phase diagram of hadronic and quark-gluon matter in the  $T - \mu$  plane. The experimental values for the chemical freeze-out are shown together with results of lattice QCD calculations, the predicted critical point is marked by the open triangle [50]. Also included are calculations of freeze-out curves for a hadron gas at constant energy density ( $= 500 \text{ MeV}/\text{fm}^3$ ) and at constant total baryon density ( $n_b = 0.12 \text{ fm}^{-3}$ ). The full triangle indicates the location of ground state nuclear matter (atomic nuclei). Right panel: schematic view of the phase diagram of nuclear matter. Also shown are the estimated trajectories of the system at current RHIC experiments, RHIC-energy-scan and future-FAIR experiments energy domains.*

quenching seem to be already confirmed by the very first LHC data from ALICE, CMS and ATLAS collaborations.

Another crucial feature is provided by the measured particle distributions. Most remarkably the systematic study of these measured yield distributions in terms of a statistical hadronization model, has revealed a universal “hadro-chemical” equilibrium, the yield distributions resembling grand canonical Gibbs ensembles of hadrons and resonances [51]. The derived parameters of the population,  $T$  and  $\mu = \mu_B$ , vary monotonously with  $\sqrt{s}$  as shown on fig. 12. The circles represent the chemical freeze-out points where the hadrons cease to interact producing the observed yield. These circles corresponds to various incident energies from SIS via AGS and SPS to RHIC, *i.e.*,  $3 \leq \sqrt{s} \leq 200 \text{ GeV}$ . The point very near zero chemical potential corresponds to the RHIC situation. We see that the freeze-out almost exactly coincides with the crossover transition. The interpretation is that the hadronization itself is statistical. The hadronization transition creates a hadron gas ensemble maximizing the entropy which exhibits a characteristic ordering pattern concerning the relative abundance of each hadronic species. In this very high energy situation the number of produced quark and antiquark partons is huge, much larger than the net quark number,  $n_q - n_{\bar{q}}$ , yielding a very low chemical potential. A very important experimental challenge is the search of the CEP. This requires a lower collision energy to increase the net baryonic density and chemical potential. This is one of the central goal of the FAIR-CBM project and of the RHIC-Energy-Scan project. It is expected that enhanced event by event fluctuations should show up when the freeze out trajectory passes in the neighboring of the CEP. Examples of such trajectories for various incident energies are shown on the right panel of fig. 12.

### 5.3 Center symmetry of QCD

We already said that chiral symmetry restoration is accompanied by the liberation of quark and gluon degrees of freedom associated with the deconfinement. One question is thus to characterize the deconfinement transition and to identify some indicators for this phenomenon. We will see that under certain

circumstances it exists a symmetry, called the center symmetry, related to the confinement/deconfinement transition. To introduce the subject we first limit ourselves to the vanishing baryonic chemical potential case. The QCD partition function reads

$$Z = \text{Tr} e^{-\beta H} = \sum_n \langle n | e^{-\beta H} | n \rangle \quad \text{with} \quad \beta = \frac{1}{T} \quad (110)$$

where the trace is evaluated by summing over all quantum states of a certain basis  $\{|n\rangle\}$ . The QCD hamiltonian  $H$  is obtained from the QCD lagrangian (8) by the standard Legendre transform. In one dimensional quantum mechanics it reads  $H(x, p) = p\dot{x} - L(x, \dot{x})$  with the conjugate momentum of the variable  $x$  defined by  $p = \partial L / \partial \dot{x}$ . In QCD the variables are the fields taken at each point  $\vec{r}$ :  $(A^\mu(\vec{r}), \psi(\vec{r}))$  for each possible color or flavor. It is important to notice that the time component of the glue field has no conjugate momentum. This is therefore not a dynamical variable. The conjugate momentum of the variable  $A_a^j$  can be identified with the chromoelectric field up to a sign :

$$\Pi_j^a \equiv \frac{\partial \mathcal{L}}{\partial A_a^j} = -G_{0j}^a = \partial_j A_a^0 + \partial_0 A_a^j - g f_{abc} A_b^0 A_c^j = -E_j^a. \quad (111)$$

We introduce the covariant derivative of the electric field defined as  $D_i^{ab} E_i^b = \partial_i E_i^a - g f_{adb} \vec{A}_d \cdot \vec{E}_b$  and the color density carried by quarks,  $\rho_a = \psi_f^\dagger \frac{\lambda_a}{2} \psi_f$ . Since the conjugate momentum,  $\Pi_a^0$ , of  $A_a^0$  has to be zero at any time, it has to commute with the hamiltonian  $H$  :

$$\frac{\partial \Pi_a^0}{\partial t} = i [H, \Pi_a^0] \equiv 0 = D_i^{ab} E_i^b - \rho_a. \quad (112)$$

The last equality comes from the explicit calculation of the commutator using canonical commutation relations. It just represents Gauss law, the difference with electrodynamics is that the charge density contains not only a matter piece ( $\rho_a$ ) but also a gluon piece ( $g f_{adb} \vec{A}_d \cdot \vec{E}_b$ ) hidden in the covariant derivative of the chromoelectric field. If these two conditions ( $\Pi_a^0 = 0$ , Gauss law) are satisfied at time  $t$ , they are valid at any time. The quantum mechanical consequence is that physical states should fulfill :

$$\Pi_a^0 |\Psi\rangle = 0, \quad (D_i^{ab} E_i^b - \rho_a) |\Psi\rangle = 0. \quad (113)$$

In quantum mechanics the usual wave function representation of the state  $|\Psi\rangle$  is  $\Psi(x) = \langle x | \Psi \rangle$  and the momentum operator is represented by  $P = -i\partial/\partial x$  acting on the wave function  $\Psi(x)$ . In the case of the gauge field theory the state  $|\Psi\rangle$  is represented by the wave function  $\Psi(A^\mu(\vec{r}), \psi(\vec{r}))$  and the conjugate momenta are represented by  $\Pi_a^\mu = -i\partial/\partial A_a^\mu$  acting on the wave function. The two conditions (113) become :

$$i \frac{\partial \Psi}{\partial A_a^0} = 0 \quad \Psi(\vec{A}(\vec{r}), \psi(\vec{r})) = \Psi\left(h\left(\vec{A} + i\vec{\nabla}\right)h^\dagger, h\psi(\vec{r})\right) \quad (114)$$

The first equation implies that the wave function does not depend on  $A_a^0$ . The second one comes from Gauss law and constitutes the quantum version of gauge invariance.

To calculate the trace in the partition function we use a basis  $\{|n\rangle = |\vec{A}(\vec{r}), \psi(\vec{r})\rangle\}$ . The partition function is thus

$$Z = \text{Tr} e^{-\beta H} = \prod_{\vec{r}} \int \mathcal{D}A(\vec{r}) \int \mathcal{D}\psi(\vec{r}) \langle A(\vec{r}), -\psi(\vec{r}) | e^{-\beta H} \delta(D_i^{ab} E_i^b - \rho_a) | A(\vec{r}), \psi(\vec{r}) \rangle$$

where the projection on physical states is performed through the introduction of a delta function,  $\delta(D \cdot E - \rho)$ , enforcing Gauss law. It can be shown by pure mathematical manipulations that the partition function admits a path integral representation

$$Z(\beta) = \prod_{\vec{r}, 0 < x_4 < \beta} \int \mathcal{D}A(\vec{r}, x_4) \int \mathcal{D}\psi(\vec{r}, x_4) \int \mathcal{D}\bar{\psi}(\vec{r}, x_4) e^{-S_F} \quad (115)$$

where  $S_E$  is the Euclidean QCD action :

$$S_E = \int_0^\beta dx_4 \int d^3r L_E(A_4, \vec{A}, \psi)(\vec{r}, x_4). \quad (116)$$

The Euclidean QCD lagrangian,  $L_E$ , is formally obtained from the Minkovski lagrangian :

$$L_E(A_4, \vec{A}, \psi)(\vec{r}, x_4) = -\mathcal{L}_M(A_0 = -iA_4, \vec{A}, \psi)(\vec{r}, x_0 = -ix_4). \quad (117)$$

It depends on the spatial point and on a pseudo-time formally obtained from the ordinary time by  $x_4 = ix_0$ . For this reason it is referred as an imaginary time formalism. The pseudo-time integration is done on the interval  $(0, \beta)$ . As a reminiscence of the trace operation the field variables should satisfy the periodic or antiperiodic boundary conditions :

$$A(\vec{r}, x_4 + \beta) = A(\vec{r}, x_4), \quad \psi(\vec{r}, x_4 + \beta) = -\psi(\vec{r}, x_4). \quad (118)$$

The minus sign for the fermion field comes from its peculiar mathematical nature : it is an anticommuting Grassman variable.

The euclidean lagrangian is also gauge invariant :

$$A_\mu \rightarrow {}^h A_\mu = h A_\mu h^\dagger - i h \partial_\mu h^\dagger, \quad \psi \rightarrow {}^h \psi = h \psi. \quad (119)$$

The gauge invariance of QCD actually requires that the action is gauge invariant. This places constraints on the allowed gauge transformations :

$${}^h A_\mu(\vec{r}, x_4 + \beta) = {}^h A_\mu(\vec{r}, x_4), \quad {}^h \psi(\vec{r}, x_4 + \beta) = -{}^h \psi(\vec{r}, x_4). \quad (120)$$

Obviously this constraint will be automatically fulfilled by periodic gauge transformations,  $h(\vec{r}, x_4 + \beta) = h(\vec{r}, x_4)$ . However besides these periodic ones, we can also find transformations which are periodic in time up to global (constant) twist transformation  $f$  :

$$h(\vec{r}, x_4 + \beta) = f h(\vec{r}, x_4) \quad (121)$$

Under such a transformation one has :

$${}^h A_\mu(\vec{r}, x_4 + \beta) = f {}^h A_\mu(\vec{r}, x_4) f^\dagger, \quad {}^h \psi_\mu(\vec{r}, x_4 + \beta) = -f {}^h \psi_\mu(\vec{r}, x_4). \quad (122)$$

By definition  $f$  is an element of the center of the gauge group,  $Z(3)$ , if it commutes with all the elements of the group :  $[f, A_\mu] = A_\mu^a [f, t_a] = 0$ . The elements of  $Z(3)$  are multiples of the unit matrix :

$$f \in Z(3) \Rightarrow f = z I \quad z = e^{2i\pi n/3} \quad n = 1, 2, 3.$$

If the twist transformation,  $f$ , belongs to  $Z(3)$ , it follows that :

$${}^h A_\mu(\vec{r}, x_4 + \beta) = f {}^h A_\mu(\vec{r}, x_4) f^\dagger \equiv {}^h A_\mu(\vec{r}, x_4), \quad {}^h \psi_\mu(\vec{r}, x_4 + \beta) = -z {}^h \psi_\mu(\vec{r}, x_4). \quad (123)$$

The important result is that the boundary conditions for the glue field are maintained after this twisted gauge transformation. Consequently the pure gauge action remains invariant. The associated symmetry is called the center symmetry. However this symmetry is broken in presence of light quarks since  ${}^h \psi_\mu(\vec{r}, x_4 + \beta) = -z {}^h \psi_\mu(\vec{r}, x_4)$ . Nonetheless, the center symmetry is useful as an approximate symmetry of QCD which becomes exact if the dynamical quarks are neglected. Note, that we stress the word ‘‘dynamical’’ in the context of quarks. Indeed, the center symmetry is an important aspect of the theory in particular in the presence of static quarks.

**Order parameter : Polyakov loop.** Let us consider the pure gauge theory and put a static (infinitely heavy) quark at point  $\vec{R}$ . the quark-gluon interacting part of the action is

$$S_Q = \int_0^\beta dx_4 \int d^3r \left( g t_a \delta(\vec{r} - \vec{R}) \right) (-iA_4^a)(\vec{r}, x_4) = -ig \int_0^\beta dx_4 A_4(\vec{R}, x_4) \quad (124)$$

which is nothing but the standard potential energy of a charge in an (chromo)-electric potential. This action has to be added to the pure gauge action,  $S_E$ . Hence the partition function of the system of gluons in presence of a static quark reads

$$Z_Q(\beta, \vec{R}) = \int \mathcal{D}[A, \psi, \bar{\psi}] e^{-S_E(\text{pure gauge})} L(\vec{R}) \quad (125)$$

where  $L(\vec{R})$  is defined as the Polyakov loop :

$$L(\vec{R}) = \frac{1}{N_c} \text{Tr}_c \exp \left[ ig \int_0^\beta dx_4 A_4(\vec{R}, x_4) \right] = \frac{1}{N_c} \text{Tr}_c \exp \left[ ig \int_0^\beta dx_4 t_a A_4^a(\vec{R}, x_4) \right]. \quad (126)$$

It is a loop since it is a Wilson line closed on itself due to the periodic boundary condition. It is gauge invariant since it is invariant under a periodic gauge transformation. The Polyakov loop is thus a color singlet which is manifest from the presence of the trace which averages over the quark colors. It has however a  $Z(3)$  charge since it is not invariant under a  $Z(3)$  transformation :

$$L(\vec{R}) \rightarrow z L(\vec{R}). \quad (127)$$

Obviously the thermal expectation value of the Polyakov loop

$$\Phi(\vec{R}) \equiv \langle L(\vec{R}) \rangle = \frac{1}{Z(\text{Gluon})} \int \mathcal{D}[A, \psi, \bar{\psi}] e^{-S_E(\text{pure gauge})} L(\vec{R}) = \frac{Z_Q}{Z(\text{Gluon})} = e^{-\beta F_Q(\vec{R})} \quad (128)$$

is just the ratio of the partition functions of the gluons system with and without the external color source. Therefore, this expectation value measures the free energy  $F$  of the static test quark. This aspect connects the center center symmetry to confinement. At low temperature color is confined and the free energy of a single isolated quarks is therefore infinitely large  $F = \infty$ . Hence in the confined phase  $\Phi = \langle L \rangle = 0$ . On the other hand, at high temperatures asymptotic freedom suggests that quarks and gluons become deconfined. There  $F$  is finite and  $\Phi = \Phi_0 \neq 0$  in the deconfined phase. From (127) we know that  $L$  transforms non-trivially under center symmetry transformations. Therefore, a non-zero expectation value,  $\Phi_0$ , implies that the  $Z(3)$  symmetry is spontaneously broken at high temperatures in the deconfined phase. Thus,  $\Phi$  qualifies as an order parameter of deconfinement in the pure gauge theory, *i.e.*, in absence of dynamical quarks. In fact, it is easy to understand why the center symmetry must break spontaneously at high temperatures. In the limit  $\beta = 1/T \rightarrow 0$ , the integral in (126) extends over shorter and shorter Euclidean time intervals and hence  $\Phi \rightarrow (Tr I)/3 = 1$ .

**Indicators for chiral symmetry restoration and deconfinement.** We have seen on one hand that in the chiral limit, the quark condensate plays the role of an order parameter associated with chiral restoration at high temperature. On the other hand, in absence of dynamical quarks, there is an exact center symmetry which is spontaneously broken in the high temperature region where quarks and gluons are deconfined, the associated order parameter being the Polyakov loop. In the real QCD neither the chiral symmetry nor the center symmetry are exactly realized but we can hope that the quark condensate and the Polyakov loop remain valid indicators of rapid chiral and deconfinement crossovers. This is confirmed by lattice calculations which clearly exhibit a sudden change of these two order parameters [52, 53]. An example of lattice results is shown on fig. 13.

## 5.4 The PNJL model

I will close this chapter by discussing a subject which has been studied by many group following the work of Fukushima [54] aiming to have a simultaneous description of chiral restoration and deconfinement a



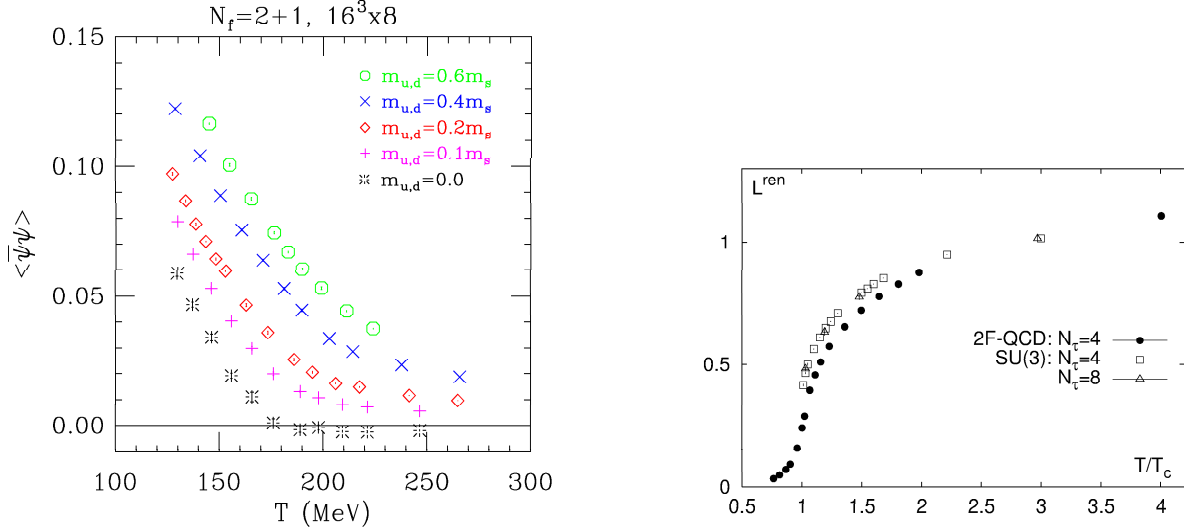


Figure 13: Left panel: the light quark condensate in QCD with 2 light up and down and a heavier strange quark mass [52]. Right panel: the Polyakov loop expectation value in the  $SU(3)$  gauge theory and in two-flavor QCD [53].

finite temperature in the whole  $(\mu, T)$  plan. The required starting point is a model description in which the vacuum possesses a quark condensate and a condensate of “Wilson line” associated with  $\Phi \neq 0$ . To incorporate both aspects simultaneously, extensions of the NJL model have been proposed by coupling the quarks to the background gauge field associated with the Polyakov loop through a covariant derivative. There are numerous works devoted to this model and I will follow here the work of ref. [55, 56] and a recent review [57]. The lagrangian of the model, named Polyakov-NJL (PNJL) model, is

$$\mathcal{L}_{NJL} = \mathcal{L}_{NJL} - i q^\dagger A_4 q - U(\Phi, T), \quad (129)$$

where  $-i q^\dagger A_4 q$  comes from the gauge part of the covariant derivative. The potential  $U(\Phi, T)$  is the effective potential of the Polyakov loop with parameters fitted to reproduce the equation of state of pure gauge lattice QCD which exhibits a deconfinement transition at  $T_0 = 270 \text{ MeV}$ . Solving the model at the mean field level is a standard thing : one first calculates the grand potential with the result :

$$\begin{aligned} \Omega(T, \mu; M, \Phi) &= U(\Phi, T) + \frac{(M - m)^2}{2G_1} - 2N_f N_c \int \frac{d^3p}{(2\pi)^3} E_p + \Omega_{QP}(T, \mu; M, \Phi) \\ \Omega_{QP}(T, \mu; M, \Phi) &= -2N_f \int \frac{d^3p}{(2\pi)^3} \left[ \ln \left( 1 + 3\Phi e^{-\beta(E_p - \mu)} + 3\Phi e^{-2\beta(E_p - \mu)} + e^{-3\beta(E_p - \mu)} \right) \right. \\ &\quad \left. + \ln \left( 1 + 3\Phi e^{-\beta(E_p + \mu)} + 3\Phi e^{-2\beta(E_p + \mu)} + e^{-3\beta(E_p + \mu)} \right) \right]. \end{aligned} \quad (130)$$

The quantity  $\Omega_{QP}$  represents the quasi-particle contribution for constituent quarks with energy  $E_p = \sqrt{p^2 + M^2}$ . The minimization of the grand potential gives the value of the constituent quark mass and of the Polyakov loop :

$$\frac{\partial \Omega}{\partial M} = 0, \quad \frac{\partial \Omega}{\partial \Phi} = 0. \quad (131)$$

In the pure gauge case the Polyakov loop is zero below the temperature  $T_0$  at which point it jumps to a finite value signaling a second or very weak first order transition. The result of such a calculation [55] is shown on the left panel of fig. 14. Also shown on the right panel is the pressure,  $P(T) = -U(\Phi, T)$ , from which the energy and entropy density can be deduced using standard thermodynamic relations. The agreement of the model with pure gauge lattice data is very good.

The next step is to compare the approach in presence of quarks with existing and safe lattice data at zero chemical potential [55]. We see on fig. 15 that the scaled pressure and the so-called interaction

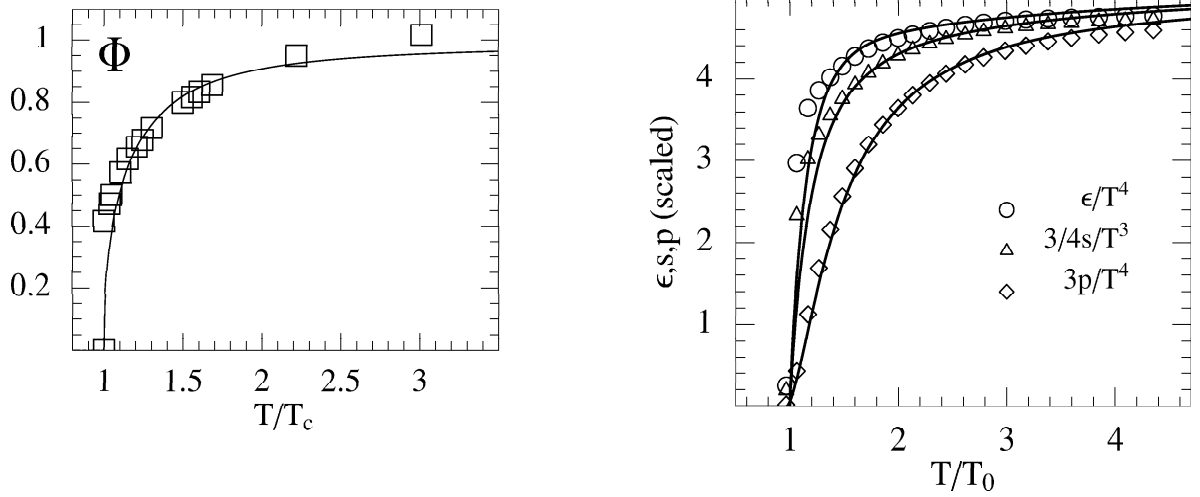


Figure 14: *Left panel: Polyakov loop as a function of temperature in the pure gauge sector, compared to corresponding lattice results. Right panel: scaled pressure, entropy density and energy density as functions of the temperature in the pure gauge sector, compared to the corresponding lattice data. Taken from [55].*

measure are in good agreement with lattice data. We observe on the right panel of fig. 15, where the chiral condensates and Polyakov loop are depicted, that the inclusion of quarks transforms the true phase transition into a continuous transition. We also note that the continuous crossovers for the quark condensate and the Polyakov loop almost exactly coincide. Other sensible quantities are the various susceptibilities. We show on the left panel of fig. 16 the results of a calculation with an improved Polyakov loop potential [56]. Again the coincidence between chiral restoration and deconfinement is very visible. Also shown are various susceptibilities related to the second derivatives of the grand potential.

The model results can be also compared with existing data at finite chemical potential. Particularly interesting quantities are the net quark number density and various susceptibilities for which lattice data exist. It is clear on fig. 17, showing the net quark number density, that the PNJL model considerably improves the simple NJL one. The origin of this improvement can be understood easily by considering

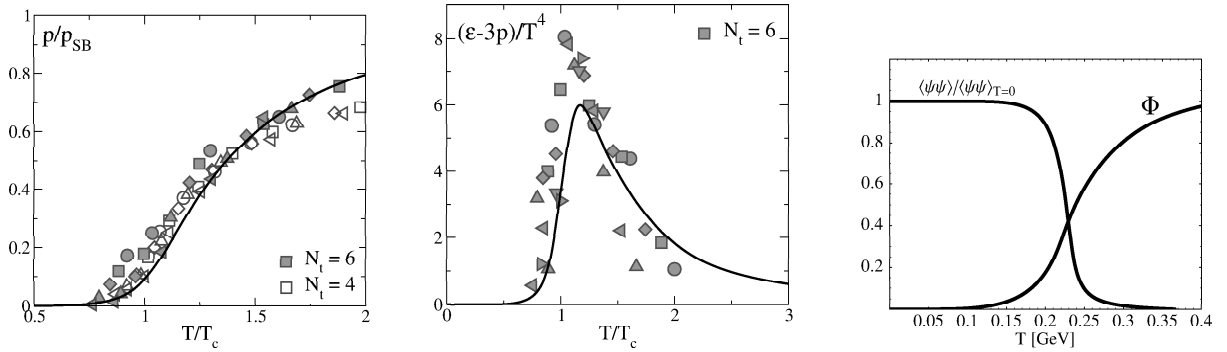


Figure 15: *Left panel: scaled pressure divided by the Stefan-Boltzmann (ideal gas) limit as a function of temperature at zero chemical potential: comparison between PNJL model prediction and lattice results. Middle panel: scaled interaction measure compared to lattice results. Right panel: scaled chiral condensate and Polyakov loop as functions of temperature at zero chemical potential. See [55] for more details.*

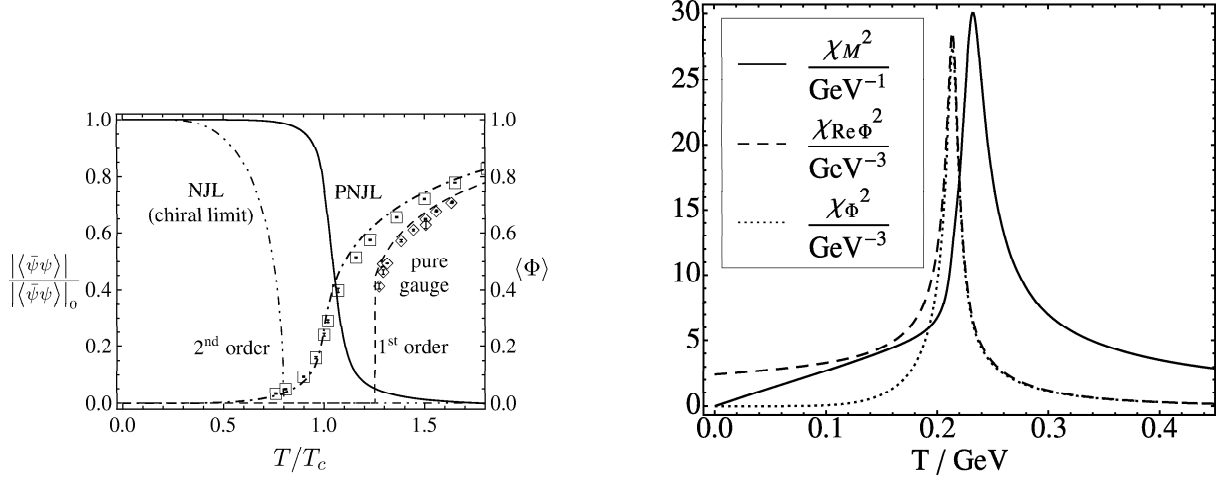


Figure 16: *Left panel: chiral condensate normalised to its value at temperature  $T = 0$  (dash-double-dotted line) in the NJL model with massless quarks, and Polyakov loop in the pure gauge model (dashed line). The PNJL model (with non-zero quark masses) shows dynamical entanglement of the chiral (solid line) and Polyakov loop (dash-dotted line) crossover transitions. For comparison lattice data for the Polyakov loop in pure gauge and full QCD (including quarks) are also shown. Right panel: the chiral susceptibility (solid line), and Polyakov loop susceptibilities (dashed line and dotted line) plotted as functions of temperature at vanishing quark chemical potential. See [56] for detailed explanations.*

the quark and antiquark occupation numbers :

$$f_p^{(q)} = \frac{\Phi e^{-\beta(E_p - \mu)} + 2\Phi e^{-2\beta(E_p - \mu)} + e^{-3\beta(E_p - \mu)}}{1 + 3\Phi e^{-\beta(E_p - \mu)} + 3\Phi e^{-2\beta(E_p - \mu)} + e^{-3\beta(E_p - \mu)}} \quad (132)$$

$$f_p^{(\bar{q})} = \frac{\Phi e^{-\beta(E_p + \mu)} + 2\Phi e^{-2\beta(E_p + \mu)} + e^{-3\beta(E_p + \mu)}}{1 + 3\Phi e^{-\beta(E_p + \mu)} + 3\Phi e^{-2\beta(E_p + \mu)} + e^{-3\beta(E_p + \mu)}}. \quad (133)$$

The quark occupation number admits the following limits

$$\text{high } T, \Phi \rightarrow 1 : f_p^{(q)} = \frac{1}{e^{\beta(E_p - \mu)} + 1}, \quad \text{low } T, \Phi \rightarrow 0 : f_p^{(q)} = \frac{1}{e^{3\beta(E_p - \mu)} + 1} \quad (134)$$

and similar ones for the antiquark case, just changing  $\mu$  into  $-\mu$ . Hence below  $T_c$ , in the low temperature domain, one and two quarks configurations decouple from the thermodynamic and only terms with three-quarks Boltzman-factor clusters survive, considerably decreasing the net quark number in agreement with lattice data. In that sense this approach generates some kind of three-quark color clustering which can be seen as precursors of baryons, although this not at all a spatial clustering. This property has been named statistical confinement.

Finally we show on fig. 18 a recent calculation of the Coimbra-Lyon group [57] for the whole phase diagram of the model in the various cases discussed above. In the realistic situation ( $m_u = m_d = 5.5 \text{ MeV}$ ,  $m_s = 140 \text{ MeV}$ ), the first order lines terminates at the CEP and is followed by a crossover. The right panel shows the baryon number susceptibility plotted against the baryon chemical potential for three different temperatures. In case of the crossover ( $T > T_{CEP}$ ) we see a sharp peak (which becomes a kink in case of  $m = 0$ ). At the CEP this peak becomes a divergence associated with a second order transition. In case of a first order transition ( $T < T_{CEP}$ ) the baryon number susceptibility gets discontinuous.

*Acknowledgments:* I thank Magda Ericson and Hubert Hansen for numerous discussions and carefull reading of the manuscript.

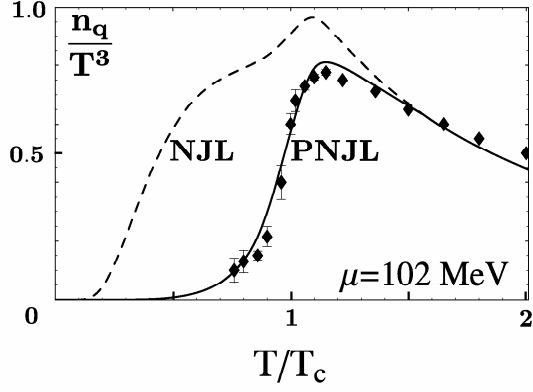


Figure 17: Comparison between the results in the PNJL model (solid line) and in the standard NJL model (dashed line) for the quark number density at  $\mu = 0.6 T_c$ . The effect of the missing confinement is evident in the standard NJL model. See [56].

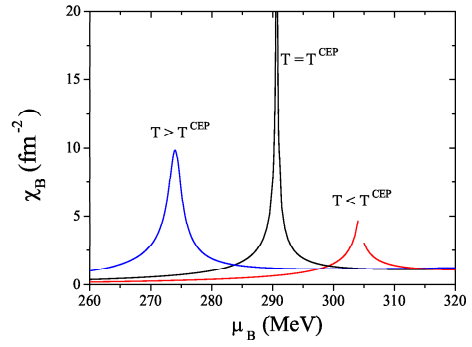
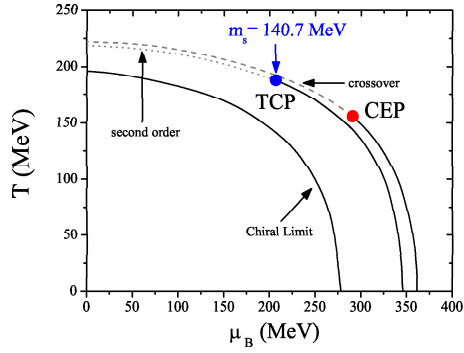


Figure 18: Left panel: the phase diagram in the SU(3) PNJL model; the solid lines represent the first order phase transition, the dotted line the second order phase transition, and the dashed line the crossover transition. Right panel: baryon number susceptibility as function of  $\mu_B$  for different temperatures around the CEP:  $T_{CEP} = 155.80$  MeV and  $T = T_{CEP} \pm 10$  MeV.

## References

- [1] FF.J. Yndurain, Quantum Chromodynamics: An introduction to the theory of quarks and gluons, Springer-Verlag, New-York.
- [2] G. Altarelli, Phys. Rept. 81 (1982) 1.
- [3] M. Gell-Mann, Phys. Lett. 8 (1964) 214.
- [4] J.C. Collins, A. Duncan and S.D. Joglekar, Phys. Rev. D16 (1977) 438. N.K. Nielsen, Nucl. Phys. B210 (1977) 212.
- [5] M.A. Shifman, A.I. Vainshtein and V.I. Zakharov, Nucl. Phys. B147 (1979) 385, 448.
- [6] A. Chodos et al, Phys. Rev. D9 (1974) 3471, D10 (1974) 2599.
- [7] F. Bissey *et al*, Nucl. Phys. B (Proc. Suppl.) 141 (2005) 22, hep-lat/0501004.
- [8] M. Gell-Mann, R.J. Oakes and B. Renner, Phys. Rev. 175 (1968) 2195.
- [9] R. Barate et al. (ALEPH collaboration) Eur. Phys. J. C4 (1998) 409.

- [10] S. P. Klevansky, Rev. Mod. Phys. 64 (1992) 649 .
- [11] M. Buballa, Phys. Rept. 407, 205 (2005), arXiv:hep-ph/0402234.
- [12] A. Bazavov et al, Phys. ReV. D80 (2009) 014504.
- [13] P.O. Bowman, U.M. Heller and A.G. Williams, Phys.Rev. D66 (2002) 014505.
- [14] D.I. Dyakonov and V.Yu Petrov, Nucl. Phys. B272 (1986) 457.
- [15] L. Ya. Glozman, Phys. Rep. 444 (2007) 1.
- [16] G. Chanfray and M. Ericson, arXiv:1011.4280 [nucl-th]; to be published in Phys. Rev. C.
- [17] M. Procura, B. Musch, T. Wollenweber, T. Hemmert and W.Weise, Phys. Rev. D 73 (2006) 114510.
- [18] D.B. Leinweber, A.W. Thomas and R.D. Young, Phys. Rev. Lett. 92 (2004) 242002.
- [19] G. Chanfray and M. Ericson, EPJA 16 (2003) 291.
- [20] G. Chanfray and M. Ericson, EPJA 25 (2005) 151.
- [21] F. Karsch, Nucl. Phys. B (Proc. Suppl.) 83 (2000) 14.
- [22] G. Chanfray and M. Ericson, Phys. Rev C75 (2007) 015206.
- [23] S. Schael et al. (ALEPH collaboration) Phys. Rep. 421 (2005) 191.
- [24] M. Dey, V.L. Eletsky and B.L. Ioffe, Phys. Lett. B252 (1990) 620.
- [25] G. Chanfray, J. Delorme, M. Ericson and M. Rosa-Clot, Phys. Lett. B455 (1999) 39.
- [26] S. Weinberg, Phys. Rev. Lett. 18 (1967) 507.
- [27] H. Leutwyler, Annals Phys. 235 (1994) 165.
- [28] V. Bernard, N. Kaiser and U.-G. Meiner, Int. J. Mod. Phys. E 4 (1995) 193 .
- [29] N. Kaiser, S. Fritsch and W. Weise, Nucl. Phys. A697 (2002) 255.
- [30] S. Fritsch, N. Kaiser and W. Weise, Nucl. Phys. A750 (2005) 259.
- [31] B.D. Serot, J.D. Walecka, Adv. Nucl. Phys. 16(1986) 1; Int. J. Mod. Phys. E16 (1997) 15.
- [32] P. Finelli, N. Kaiser, D. Vretenar and W. Weise, Nucl. Phys. A770 (2006) 1.
- [33] K.G. Wilson, Phys. Rev. 179 (1969) 1499.
- [34] M. Ericson and T.E.O. Ericson Annals of Physics 36 (1966) 323.
- [35] G. Chanfray, Z. Aouissat, P. Schuck and W. Norenberg, Phys. Lett. B256 (1991) 325.
- [36] P. Guichon and J. Delorme, Phys. Lett. B263 (1991) 157.
- [37] Z. Aouissat, R. Rapp, G. Chanfray, P. Schuck and J. Wambach, Nucl. Phys. A581 (1995) 471.
- [38] J.G. Messchendorp *et al.*, Phys. Rev. Lett. 89, 222302 (2002).
- [39] L. Roca, E. Oset and M.J. Vicente Vacas, Phys. Lett. B541 (2002) 77.
- [40] G. Chanfray and P. Schuck, Nucl. Phys. A555 (1993) 329.
- [41] G. Chanfray, R. Rapp and J. Wambach, Phys. Rev. Lett. 76 (1996) 368.
- [42] R. Rapp, G. Chanfray and J. Wambach, Nucl. Phys. A617 (1997) 472.

- [43] R. Rapp and J. Wambach, Adv. Nucl. Phys. 25 (2000) 1.
- [44] R. Rapp, J. Wambach and H. van Hees, arXiv:0901.3289 [hep-ph].
- [45] R. Arnaldi et al, (NA60 collaboration) Phys. Rev. Lett. 96 (2006) 0162302; Eur. Phys. J. C61 (2009) 711.
- [46] H. van Hees and R. Rapp, Phys. Rev. Lett. 97, (2006) 102301.
- [47] T. Hilger, R. Thomas, B. Kampfer and S. Leupold, arXiv:1005.4876 [nucl-th].
- [48] M. Stephanov, PoSLAT2006:024,2006, arXiv:hep-lat/0701002.
- [49] Y. Aoki et al, J. High Energy Phys. 06 (2009) 088.
- [50] Z. Fodor and S.D. Katz, J. High Energy Phys. 04 (2004) 050.
- [51] A. Andronic, P. Braun-Munzinger, J. Stachel, Phys. Lett. B673 (2009) 142.
- [52] C. Bernard et al., Phys. Rev. D71,(2005) 034504.
- [53] O. Kaczmarek, F. Zantow, Phys. Rev. D71 (2005)114510 .
- [54] , K. Fukushima, Phys. Lett. B591(2004) 277.
- [55] C. Ratti, M.A. Thaler and W. Weise, Phys. Rev. D73 (2006) 014019
- [56] S. Rossner, T. Hell, C. Ratti and W. Weise, Nuclear Physics A814 (2008) 118.
- [57] P. Costa, M. C. Ruivo, C. A. de Sousa and H. Hansen, Symmetry 2(3), (2010) 1338, arXiv:1007.1380 [nucl-th].